
Linearisation of multiple RF-power amplifiers with the presence of antenna crosstalk

Based on measurement

Master thesis
Karsten Schou Nielsen

Aalborg University
Department of Electronic Systems
Fredrik Bajers Vej 7B
DK-9220 Aalborg



AALBORG UNIVERSITY

STUDENT REPORT

Department of Electronic Systems

Fredrik Bajers Vej 7

DK-9220 Aalborg Ø

<http://es.aau.dk>

Title:

Linearisation of multiple RF-power amplifiers with the presence of antenna crosstalk

Theme:**Project Period:**

2019

Project Group:**Participant(s):**

Karsten Schou Nielsen

Supervisor(s):

Ming Shen

Copies: 0**Page Numbers:** 57**Date of Completion:**

May 29, 2019

Abstract:

This project is aiming on linearisation on RF-power amplifiers with the presence of antenna cross-talk. The crosstalk plays an important role in driving the amplifiers in the linear region and therefore a better understanding of this is given by the use of measurement. First Digital Pre Distortion (DPD) is applied to one amplifier and then several amplifiers with one antenna each. The measurement shows that the antennas introduces distortion and that it can be compensated for by treating the setup with antennas as one model when doing DPD.

The content of this report is freely available, but publication (with reference) may only be pursued due to agreement with the author.



AALBORG UNIVERSITET

STUDENTERRAPPORT

Institut for Elektroniske Systemer

Fredrik Bajers Vej 7

DK-9220 Aalborg Ø

<http://es.aau.dk>

Titel:

Linearisering af flere RF-power forstærkere med indvirkning fra crosstalk mellem antenner

Tema:**Projektperiode:**

2019

Projektgruppe:**Deltager(e):**

Karsten Schou Nielsen

Vejleder(e):

Ming Shen

Oplagstal: 0**Sidetal:** 57**Afleveringsdato:**

29. maj 2019

Abstract:

Hoved formålet med denne afhandling er at undersøge hvilken indvirkning crosstalk mellem flere antenner har på RF-power forstærkere når de bliker kompenseret for deres ulinearitet med Digital Pre Distortion (DPD).

Rapportens indhold er frit tilgængeligt, men offentliggørelse (med kildeangivelse) må kun ske efter aftale med forfatterne.

Contents

| | |
|--|-----------|
| Preface | xi |
| 1 Introduction | 1 |
| 2 Basic Theory | 3 |
| 2.1 Non-linearity | 3 |
| 2.2 AM/AM and AM/PM distortion | 7 |
| 2.3 Efficiency | 8 |
| 2.4 Antenna Diversity and MIMO | 8 |
| 2.5 Array factor | 10 |
| 3 Amplifier modelling | 13 |
| 3.1 Pre-distortion | 13 |
| 3.2 DPD models | 13 |
| 3.3 Crosstalk | 17 |
| 4 Measurement | 21 |
| 4.1 Amplifier | 21 |
| 4.2 One amplifier one antenna | 24 |
| 4.3 Two amplifiers two antennas | 26 |
| 4.4 Four amplifiers four antennas | 31 |
| 4.5 Two amplifiers different current | 35 |
| 5 Antenna measurement | 39 |
| 5.1 Single antenna | 39 |
| 5.2 Two antennas | 41 |
| 5.3 Four antennas | 44 |
| 5.4 Single element four antennas | 49 |
| 6 Conclusion | 53 |
| Bibliography | 55 |
| A Antenna measurements | 57 |

Todo list

Preface

Here is the preface. You should put your signatures at the end of the preface.

Aalborg University, May 29, 2019

Author 1
<username1@XX.aau.dk>

Author 2
<username2@XX.aau.dk>

Author 3
<username3@XX.aau.dk>

Chapter 1

Introduction

This master thesis is aiming at the linearization of Power amplifiers with the presence of cross talk in antenna arrays. The tasks include - the characterization of the cross talk and its impact on the system linearity - digital pre-distortion of PAs under effects of antenna cross talks. The project is motivated by the quickly growing need from the mobile communication industry, where highly integrated beam-steerable arrays consisting of a big number of power amplifiers and antenna elements are considered as the solution for higher data rates desired in emerging applications such as self-driving cars, remote e-health etc. There will be use DPD techniques that can capture the total nonlinearity of the whole array including the PAs and antenna elements. The special focus is to reduce the system complexity, while maintaining the linearisation performance.

This project will be conducted in a way combining mainly measurements together with computation in MATLAB

Chapter 2

Basic Theory

2.1 Non-linearity

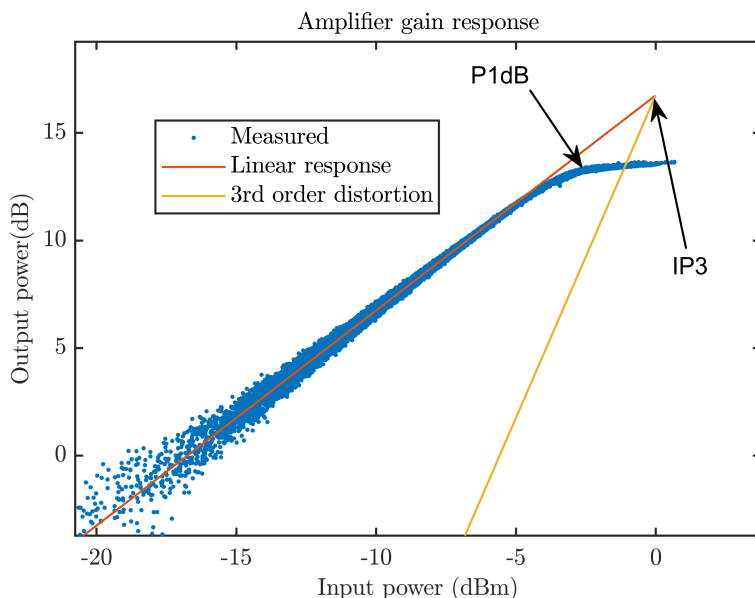


Figure 2.1: Amplifier non-linearity

An ideal power amplifier has a linear response over all frequencies and input power. This is depicted in 2.1 as Linear response. Unfortunately this is not true and therefore a measurement of a power amplifier has been done. The measurement shows that the amplifier at some level can be assumed linear, but at a point the amplifier will saturate due to the supply voltage and the gain will compress. The point where there is 1dB from the linear response to the real response is called the 1dB compression point (P1dB) which is also depicted in the figure. The non-linear gain response causes a distortion at the output which can be described by equation 2.1 [National

Instruments, 2019]. If a input-signal using two tones is considered then there will be a difference and a sum of the frequencies presented at the output which is caused by the cubic term in equation 2.3.

$$V_{out} = a_0 + a_1 V_{in} + a_2 V_{in}^2 + a_3 V_{in}^3 + a_4 V_{in}^4 + \dots \quad (2.1)$$

Where V_{out} is the output signal from the amplifier, $a_1, a_2, a_3\dots$ is coefficients describing the ratio of the distortion and V_{in} is the input signal. If a single tone input is presented, then the output will consist of purely odd and even harmonic distortion.

$$V_{in} = \sin(\omega_1 t) + \sin(\omega_2 t) \quad (2.2)$$

$$V_{out} = a_0 + a_1(\sin(\omega_1 t) + \sin(\omega_2 t)) + a_2(\sin(\omega_1 t) + \sin(\omega_2 t))^2 + a_3(\sin(\omega_1 t) + \sin(\omega_2 t))^3 + \dots \quad (2.3)$$

This is also called Two-Tone Third-Order Intermodulation Distortion and is also depicted in figure 2.1 as 3rd order distortion with a slope of 3:1. It can bee seen that when the output power increases then the 3rd order distortion increases 3 times. A measurement of this is called the third-order-intercept-point (IP3 or TOI). However, the intercept point it not directly measurable since the amplifier reaches compression way before. It can bee seen from figure 2.2 that the distorted component are spaced too close in frequency to be effectively filtered. This will cause distortion into nearby channels and is measured as Adjacent Chennel Power Ratio (ACPR).

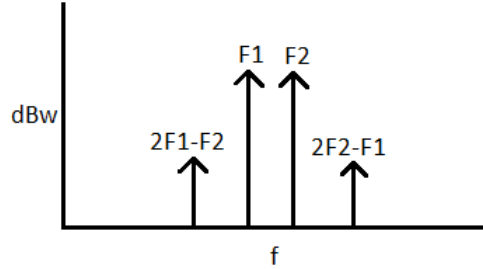


Figure 2.2: Two-Tone Third-Order Intermodulation Distortion

Distortion due to non-linearity

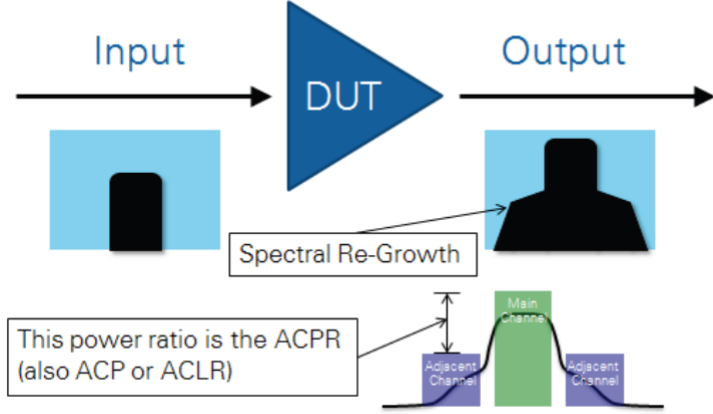


Figure 2.3: Graphical Depiction of ACPR in the frequency domain [National Instruments, 2019]

Due to the non-linearity of the PA described before, spectral regrowth will occur which will affect nearby channels. The Adjacent Channel Power Ratio (ACPR) is a measure of the power of the distortion components, caused by the non-linearity of the PA, that are leaked into the adjacent channel see figure 2.3. The formula for the ACPR is given by equation 2.4 and is used after a Fourier transform has been performed at the output signal of the PA.

$$ACPR = \frac{\int_{adjch} |Y(f)|^2 df}{\int_{mainch} |Y(f)|^2 df} \quad (2.4)$$

Where $Y(f)$ is the Fourier transform of the signal, adjch is the adjacent-channel and mainch is the main-channel.

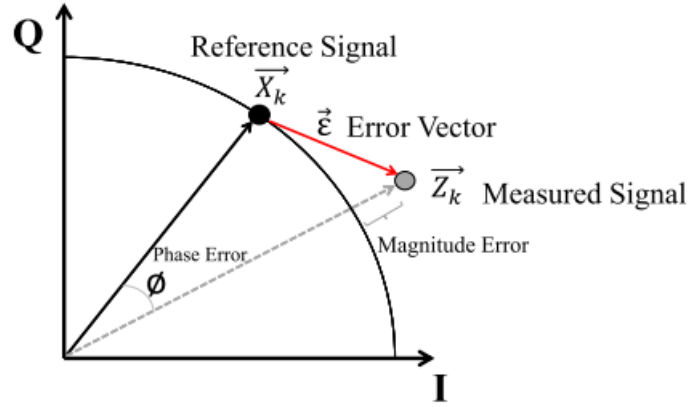


Figure 2.4: Graphical view of the EVM

Another measure of the error is the Error Vector Measurement (EVM) or Relative Constellation Error (RCE) which both is a measure of the error due to the constellations points in a IQ plot. If a signal is sent through an amplifier with a given IQ value, then the amplifier will distort those IQ values. The EVM and RCE is a measure of the power of the error vector divided by the power of the reference vector. [Ali Cheaito, et. al, 2016]

$$EVM = \frac{P_{error}}{P_{reference}} = \frac{E[|z(t) - x(t)|^2]}{E[|x(t)|^2]} \quad (2.5)$$

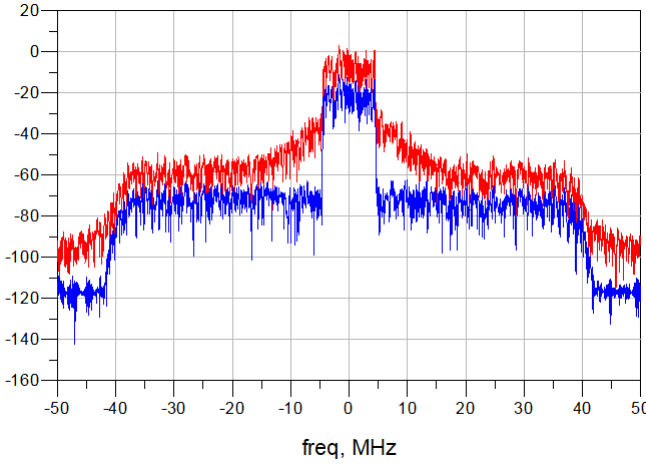


Figure 2.5: Destortion simulated in ADS, where blue is input-signal and red is output-signal. The simulation is made with a single amplifier connected to a 50Ω resistor. It is clearly that the output-signal is distorted. The ACPR becomes -45dB with a BW at 10MHz

2.2 AM/AM and AM/PM distortion

If the input signal to the PA is modelled as equation 2.6

$$x(t) = a(t)e^{j\phi(t)} \quad (2.6)$$

Where $a(t)$ is the envelope of the signal and $e^{j\phi(t)}$ is the phase of the input signal. Then the distorted output of the amplifier will be that of equation 2.6 where $g(t)$ is the amplitude distortion and $f(t)$ is the phase distortion also called Amplitude to Amplitude (AM/AM) and Amplitude to Phase (AM/PM) distortion. AM/AM distortion can be defined as the deviation from the constant gain when PA is operated in compression region. On the other hand, the increased phase change at compression region can be termed as AM/PM distortion. In presence of wideband signals having non constant amplitude, PA behaves as nonlinear system and exhibits two types of non-linearities which is static distortion and memory effects.

$$y(t) = g(a(t))e^{j\phi(t)+f(a(t))} \quad (2.7)$$

Memory effects

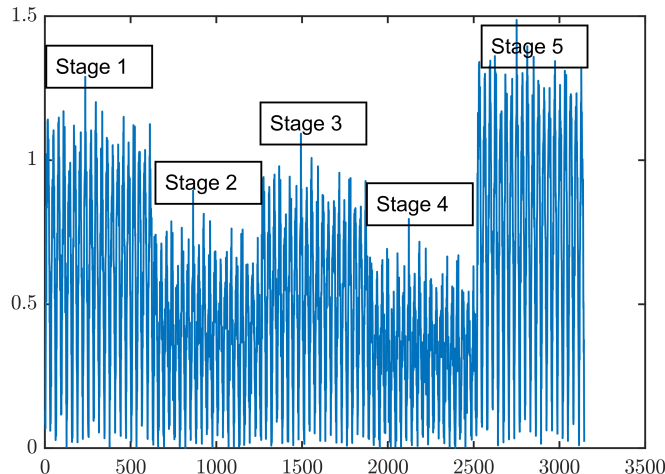


Figure 2.6: Example of amplitude changes at the input of a PA

In modern communication systems, the input power to the PA may be adjusted corresponding to the needs by the network. This makes a sudden increase or decrease in the power as depicted in figure 2.6 which makes the PA work in the transient stage [Yan Guo, et.al, 2015] [Taijun Liu, et.al, 2007]. The transient stage is where the power suddenly increases or decreases to another mean power, whereas the steady state is when the PA operates under stable conditions where the mean power

is constant. When the PA is operated in steady state under a high mean power, the amplifier will begin to dissipate heat. This will cause the internal transistors to operate under a hot state where the characteristic of the transistors will change due to a colder state. If the mean power suddenly is decreased the amplifier will still be hot, but with time the amplifier will cool down and the characteristic will change. This can be called slow memory effects whereas fast memory effects is when the amplifier is driven in its steady state and the parasitics of the components distort the signal. Also antennas at the output of the amplifier has an important role specially if several antennas are connected to form an array. The electrical field will couple to each other and cause fields that will affect the memory effects in the system.

2.3 Efficiency

An important measure of an amplifier is its efficiency, specially when the amplifier is located in a battery powered application. The efficiency of a amplifier is given by equation 2.8

$$\eta = \frac{P_{out}}{P_{amplifier} + P_{out}} = \frac{P_{out}}{P_{DC}} \quad (2.8)$$

Where P_{out} is output power from the amplifier, $P_{amplifier}$ is power dissipated in the amplifier and P_{DC} is the power DC consumption. A more common way to express the efficiency is in terms of power added efficiency (PAE) which is a measure of the difference of power between the output and the input signals versus the DC power consumption.

$$PAE = \frac{P_{out} - P_{in}}{P_{DC}} \quad (2.9)$$

2.4 Antenna Diversity and MIMO

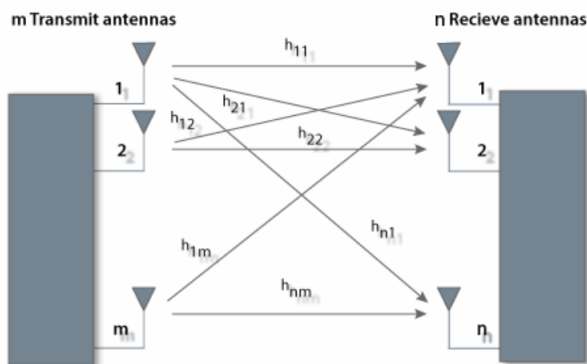


Figure 2.7: Concept of MIMO [Silvus Technologies, 2019]

MIMO (Multiple Input Multiple Output) systems are systems with Multiple Element Antennas at both link ends. The antenna elements of a MIMO system can be used for four different purposes: beamforming, diversity, interference suppression, and spatial multiplexing which is transmission of several data streams in parallel that allows improvement of capacity.[Andreas F. Molisch, 2011] A MIMO system is modelled as in equation 2.10 and is also depicted in figure 2.7.

$$\mathbf{y} = \mathbf{H}\mathbf{x} + \mathbf{n} \quad (2.10)$$

Where \mathbf{y} is the received vector, \mathbf{H} is the channel matrix, \mathbf{x} is the transmitted vector and \mathbf{n} is noise. The principle of MIMO is to ensure that the same information reaches the receiver on several statistically independent channels. In MIMO systems, several transmits paths is archived by use of several antennas, which gives a spatial separation if they are separated enough to give a correlation factor ρ that is below $0.5 - 0.7$ [Andreas F. Molisch, 2011]. The formula for the envelope correlation factor between two antennas is given by equation 2.11. The formula assumes that the WSSUS (Wide-Sense Stationary Uncorrelated Scattering) model is valid, no LOS exists, the power delay profile has an exponential shape, the incident power is isotropically distributed in azimuth and only propagates in the horizontal plane, and an omni-antenna is used.

$$\rho = \frac{J_0^2(k_0 v \tau)}{1 + (2\pi)^2 S_\tau^2 (f_2 - f_1)^2} \quad (2.11)$$

Where J_0 is the Bessel function of the first kind and S_τ is the delay-spread of the channels. If the correlation between two antennas is investigated for the same frequency, then the formula can be rewritten as equation 2.12 because $f_2 - f_1 = 0$.

$$\rho = J_0^2(2\pi d)^{-1} \quad (2.12)$$

Where d is the element spacing given in wavelengths. A plot of this can bee seen in figure 2.8.

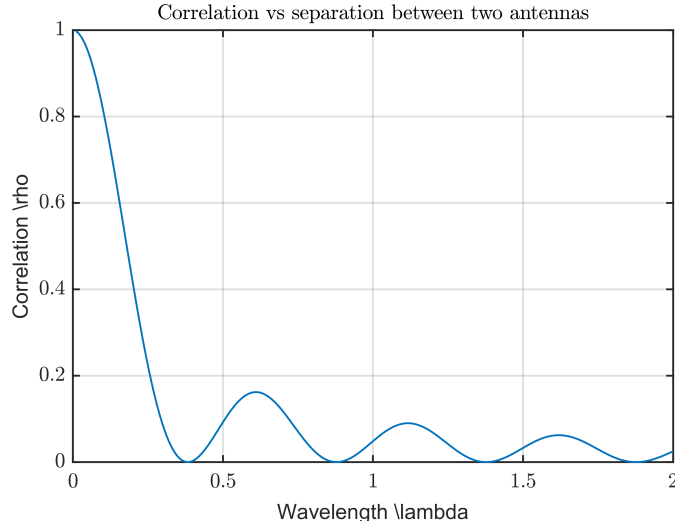


Figure 2.8: Correlation factor for two antennas versus distance

Another method to calculate the correlation factor is to use measured or simulated S-parameters as shown in equation 2.13 [Xuan Wang, et. al, 2011] where k is the propagation constant and d the distance in meters.

$$\rho = \frac{A + BJ_0(kd)}{B + AJ_0(kd)} \quad (2.13)$$

$$A = -2Re(S_{12}^*(1 - S_{11})) \quad (2.14)$$

$$B = |1 - S_{11}|^2 + |S_{12}|^2 \quad (2.15)$$

2.5 Array factor

When several antennas are spaced relatively close to each other it is called an antenna array. If the antennas are isotropic and are spaced with a quarter wavelength then the array will radiate twice the energy in the direction perpendicular to the array, thou the gain along the array will become zero. A mathematical expression of this is called the array factor (AF).

$$AF = \sum_{n=1}^N e^{(nJ2\pi d \cos(\alpha) + JB(n))} \quad (2.16)$$

Where N is number of antennas in the array, d is the distance between the antennas, α is the azimuth angle from $0..2\pi$ and B is the feeding phase of a single antenna. In figure 2.9 and 2.10 the array factor for 2 and 4 antennas spaced $[0.1, 0.2, 0.3, 0.4, 0.5, 0.6]\lambda$ are plotted respectively. It is seen that the energy doubles

in the 90° for all distances in figure 2.9 while it becomes 4 times greater in figure 2.10.

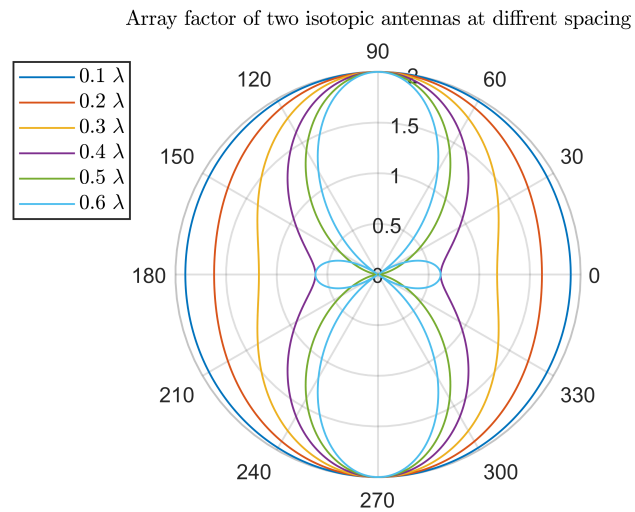


Figure 2.9: Array factor of two antennas with different spacing

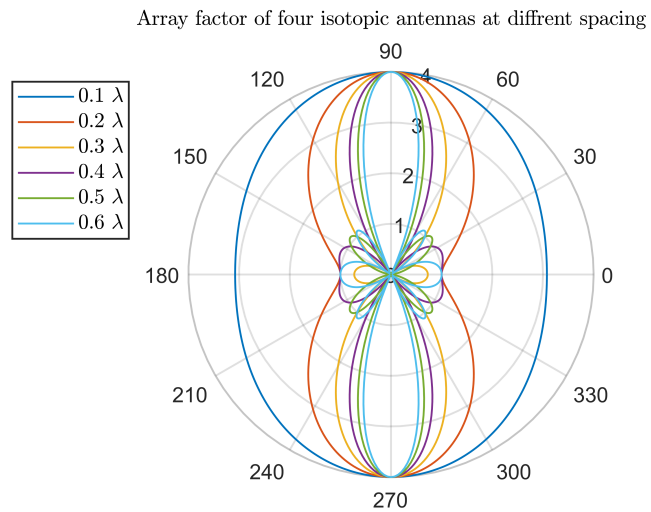


Figure 2.10: Array factor of four antennas with different spacing

Chapter 3

Amplifier modelling

3.1 Pre-distortion

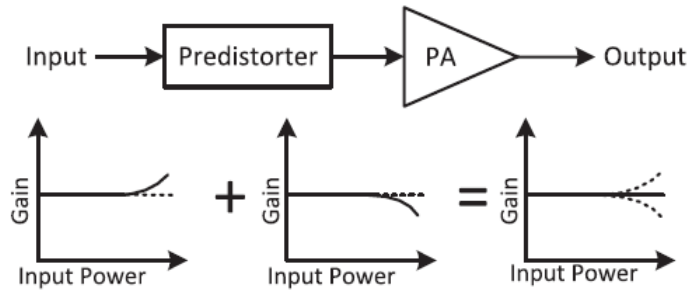


Figure 3.1: Concept of predistortion [Yan Guo, et.al, 2015]

In figure 3.1 the concept of Digital Pre-Distortion (DPD) is depicted. DPD is a way to "distort" the incoming signal with the inverse transfer-function of the amplifier. For example the gain of the amplifier is ideally linear in the small-signal region and gets non-linear at higher signal levels. To overcome this, a block called the predistorter inverses this non-linear curve which is the exact inverse of the PA, then a linear amplification can be achieved at the final PA output. But to achieve this inverse of the PA all the non-linear effects has to be accounted for including memory effects.

3.2 DPD models

Weiner

A simple model to include memory effects is the Weiner model, which consists of a linear filter $h(m)$ followed by a_k which is the polynomial coefficients of the non-linearity. The model is given by equation 3.1

$$y_{wiener}(n) = \sum_{k=1}^K a_k \left[\sum_{m=0}^{M-1} h(m)x(n-m) \right]^k \quad (3.1)$$

It is seen that the output consists of the sum of the non-linear response multiplied with the sum of the input with the former input multiplied with a filter. The Weiner model is one of the simplest ways to combine memory effects with non-linearity but unfortunately it does not provide good results for modelling a power amplifier.

Hammerstein

Another simple model is the Hammerstein model which is given by equation 3.2

$$y_{hammerstein}(n) = \sum_{m=0}^{M-1} g(m) \sum_{k=1}^K a_k x^k(n-m) \quad (3.2)$$

Which is formed by a non-linearity followed by a linear filter. It is seen that the output consist of the sum of the linear filter $g(m)$ multiplied with the sum of the filter coefficients a_k multiplied with the input signal and the former input signal in the power of k . Yet this filter is simple it does also have it's limitations when it come to modelling of power amplifiers.

Memory Polynomial

A more used and general model is the memory polynomial given in equation 3.3. The model is a deviation of the Hammerstein model which has proven effective for predistortion of actual power amplifiers under typical operations.

$$y_{mp}(n) = \sum_{k=0}^{K-1} \sum_{m=0}^{M-1} a_{km} x(n-m) |x(n-m)|^k \quad (3.3)$$

where a_{km} is the filter coefficients, $x(n)$ is the input, M is the memory debt and k is the envelope order.

Estimation of coefficients

A way to calculate the coefficients for a DPD algorithm is by use of the least-square-type algorithms. The reason for this is that the coefficients are linear weighting of non-linear signals. The easiest way to formulate such a problem is to first collect the coefficients into one $J \times 1$ vector denoted \mathbf{w} , where J is the total number of coefficients. The input can then further be assembled in to a vector denoted \mathbf{X} which dimensions is $N \times J$. The model output can then be expressed by:

$$\hat{\mathbf{y}} = \mathbf{X}\mathbf{w} \quad (3.4)$$

where $\hat{\mathbf{y}}$ is an $N \times 1$ vector which is an estimate of the real output \mathbf{y} . The inverse of this model used for predistortion is then:

$$\hat{\mathbf{x}} = \mathbf{Y}\mathbf{w} \quad (3.5)$$

where the input now is being estimated from the output samples. It is then possible to use the least-squares solution to minimize the estimation error:

$$\mathbf{w} = (\mathbf{Y}^H \mathbf{Y})^{-1} \mathbf{Y}^H \mathbf{x} \quad (3.6)$$

where \mathbf{Y} is a $J \times N$ matrix where N is number of samples. The equation can further be rewritten as:

$$\mathbf{Y}^H \mathbf{Y} \mathbf{w} = \mathbf{Y}^H \mathbf{x} \quad (3.7)$$

This equation can easily be solved by MATLAB using the "backslash" operator (\) by Cholesky decomposition and forward/backward substitution.

Estimation in MATLAB

If an input and output signal is measured and imported into MATLAB and called \mathbf{x} and \mathbf{y} respectively, then a for-loop can do the \mathbf{Y} matrix. Next we need to remove M sampels from \mathbf{x} because of the time delay, then the substitution to find \mathbf{w} using the (\) operator can be done. The code is given below:

```
K = 5;%envelope order
M = 8;%memory debth

Y = [];% init matrix
for m = 1:M
    for k = 1:K
        Y(:, end+1) = (y(m: end-M+m).* abs(y(m: end-M+m)).^(k-1));
    end
end

w = Y\y(M: end);%Do the regression
x_est = Y*w;%estimated input
error = mean(abs(x(M: end)-x_est))
```

Now equation 3.5 must be used to obtain the inverse model:

```
X = [];% init matrix
for m = 1:M
    for k = 1:K
        X(:, end+1) = (x(m: end-M+m).* abs(x(m: end-M+m)).^(k-1));
    end
end

x_inv = X*w;%inverse model
```

In figure 3.2 a AM/AM plot is depicted of measurements done at an amplifier. The plot shows how the output (blue) is driven in its non-linear region. Then the inverse model (red) inverses this non-linearity and when this signal is presented at the input of the amplifier, then the response will become close to linear (yellow). The reason that it still reaches some level of compression is because of the limit of the supply-voltage to the amplifier. A PSD of the same measurements is depicted in figure 3.3. From that it is easy to see how the pre-distorted signal lowers the distortion. From figure 3.4 a plot of the absolute value of the I and Q baseband values is depicted. It is clearly seen that the output is a non-linear response of the input and that the inverse model is compensating for the gain error.

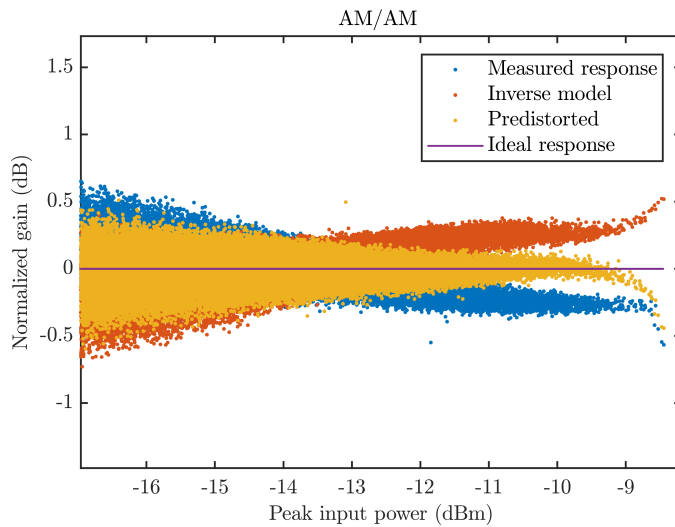


Figure 3.2: AM/AM plot of measured response and inverse model

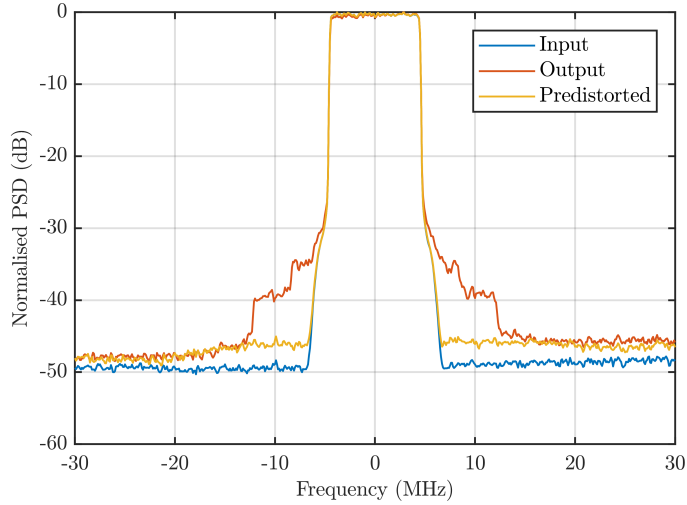


Figure 3.3: PSD of output measured at amplifier close to it's compression point and output at same power level but with predistortion.

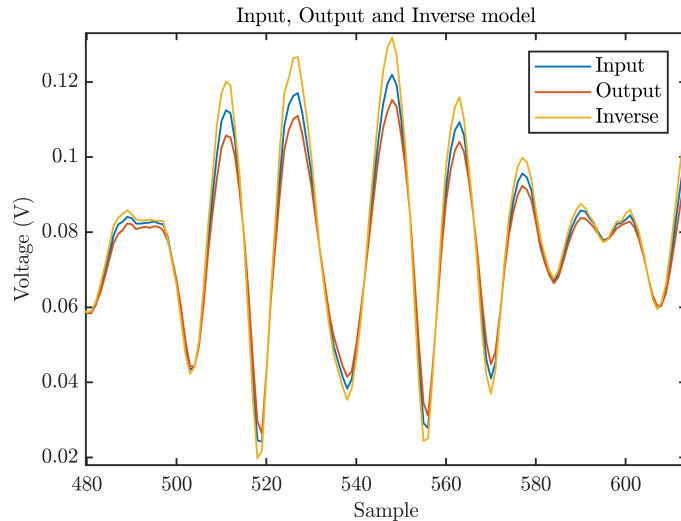


Figure 3.4: Absolute value of baseband I and Q values

3.3 Crosstalk

Crosstalk is coupling from one branch to another branch. When only a signal is present on a single branch, no crosstalk would appear to this branch. On the other hand if a signal is presented at two branches then crosstalk would appear to both of them. There exist three types of crosstalk which is: Crosstalk before the PA's, see figure 3.5, Crosstalk after the PA's, see figure 3.6 and Crosstalk on the antennas and

mishmash due to coupling. Crosstalk before the PA is also called nonlinear since it is amplified by the non linear PA. The nonlinear crosstalk and the PA nonlinear response should be jointly compensated by a predistorter to get a reliable system performance [Zahidul Islam Shahin, et. al, 2017] denoted $\mu_k(\cdot)$. The output from the branches would become that of equation 3.8.

$$Y_{1k} = fk(uk(X_{11}, X_{12}, X_{13}, X_{1k})) \quad (3.8)$$

Where X is the input signal, Y is the output and fk is the PA response.

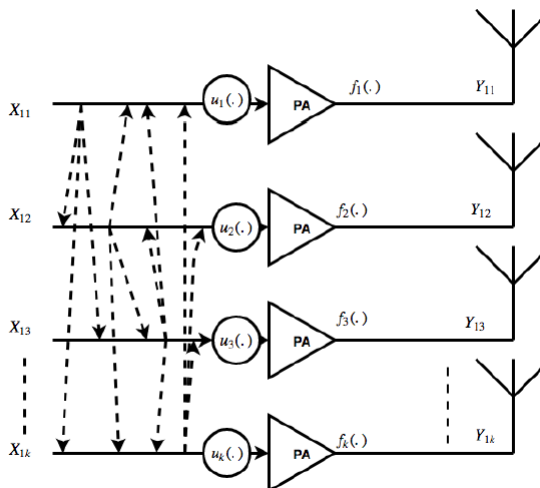


Figure 3.5: Crosstalk before PA [Zahidul Islam Shahin, et. al, 2017]

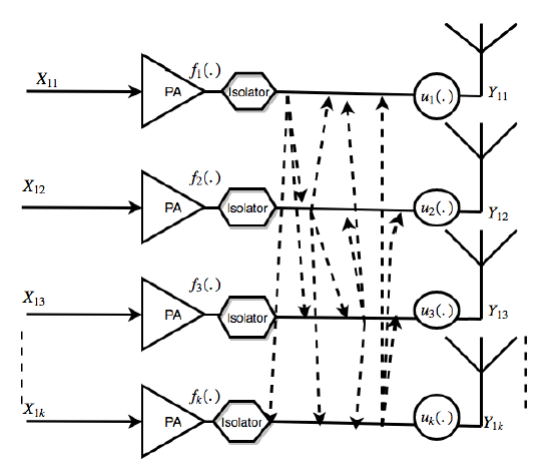


Figure 3.6: Crosstalk after PA [Zahidul Islam Shahin, et. al, 2017]

Crosstalk after the PA is called linear since it has an linear impact. In figure 3.6 the output of the amplifier is connected to an isolator, which makes the output unaffected by reflections. A linear model can therefore be used which is shown in equation 3.9.

$$Y_{1k} = \mu_k(f1(X_{11}), f2(X_{12}), f3(X_{13})..fk(X_{1k})) \quad (3.9)$$

When no isolators is presented the output will now be affected by the crosstalk or mutual-coupling between the antennas. A sketch of this is depicted in figure 3.7 where a_{1k} is the incoming signal to the amplifier, b_{2k} is the output from the amplifier and a_{2k} is the reflected signal form the antenna array at the k'th branch [Katharina Hausmair, et. al, 2017]. The relation between a_{2k} and the output signals b_{2k} is determined by the characteristics of the antenna arrays S-parameters. The system model of the multi-antenna transmitter can, therefore, be split in to a crosstalk and mismatch model (CTMM). This block can further be used together with a dual-input-DPD which holds the model for the PA, see figure 3.8.

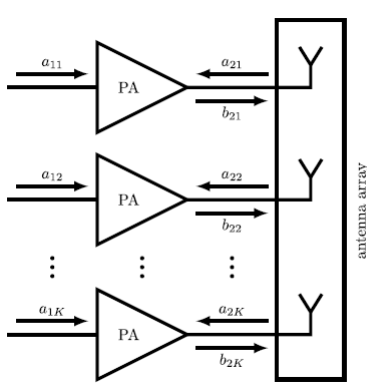


Figure 3.7: Model of the antenna crosstalk [Katharina Hausmair, et. al, 2017]

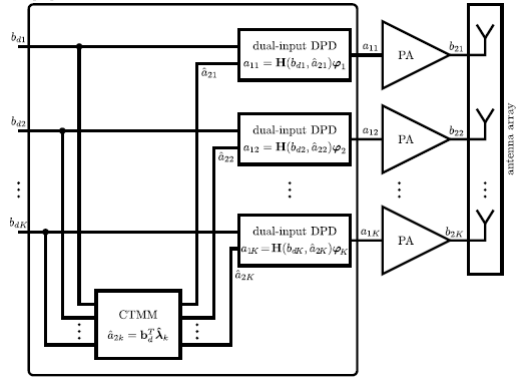


Figure 3.8: The predistortion method consists of two main blocks: one linear CTMM block for the whole transmitter and a dual-input DPD block in every transmit path. [Katharina Hausmair, et. al, 2017]

The CTMM describe the crosstalk and mishmash signals a_{2k} as a function of the PA output b_{2k} . A mathematical model of this is shown in equation 3.10.

$$a_{2k} = \sum_{i=1}^K \lambda_{ki} b_{2i} = \mathbf{b}_2^T \boldsymbol{\lambda}_k \quad (3.10)$$

Where $\mathbf{b}_2 = [b_{21}, \dots, b_{2K}]^T$ are complex coefficients describing the input to the antenna and $\boldsymbol{\lambda}_k = [\lambda_{k1}, \dots, \lambda_{kK}]^T$ are complex coefficients describing the reflection from the antenna, which also corresponds to S-parameters. The Dual-Input PA Model is then a function of the signals a_{1k} and a_{2k} which becomes a lengthy equation that is not further described here. The model can be found in [Katharina Hausmair, et. al, 2017]. Its has been found that the approach is capable of reducing the ACPR of a measurement setup using 4-Tx antennas from -36.3dB to -50.7dB which is nearly distortion free. The problem with the model is that the S-parameters for the antennas has to be known and that the method needs feedback from each amplifier. This is a large problem if several amplifiers are used since it will increase complexity in the layout and also if the S-parameters cannot be measured it introduces an other problem. A solution to this problem can be to treat the amplifiers with antennas as one amplifier and then do the DPD at the receiver side as depicted in figure 3.9. In order to make this configuration to work, the transmitter side has to send a pilot sequence to the receiver that is known for the receiver. Then the receiver can obtain the coefficients for the DPD algorithm and then do the estimation of the signal. The benefits with this approach is that also the channel is taken into account. Another problem that is omitted with this approach is that when doing DPD in the conventional way, the amplifier has to act identical to the pre distorted signal that it did to the non-distorted which not always become true.

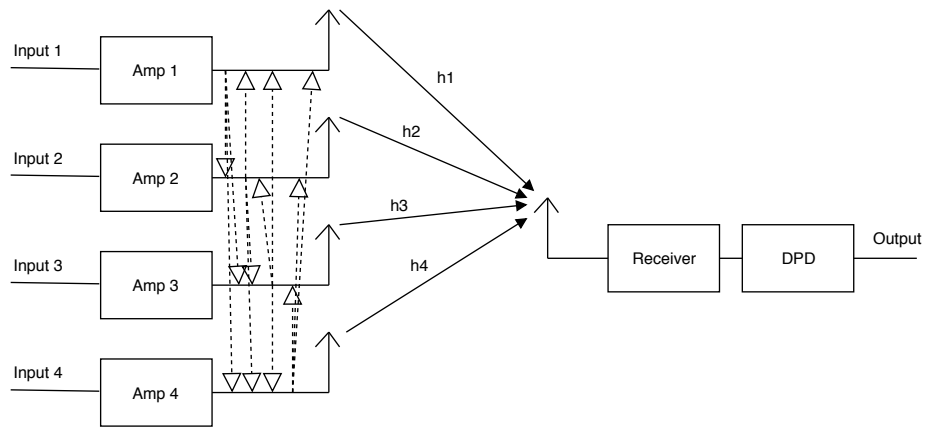


Figure 3.9: (Post)Digital Pre Distortion at receiver side. Here also the channels are taken into account.

Chapter 4

Measurement

4.1 Amplifier

The amplifier used for measurements is a CGH400006P 6W RF Power GaN HEMT transistor mounted at a development board for this transistor type, driven in class AB. The Transistor has a specified mean gain at 13dB and a maximum output at 32dBm which gives a maximum input at 19dBm. This is a large amount of power to deliver for a signal generator so in order to protect the equipment an amplifier has been connected to the output. With cable loss taken into account the amplifier has a gain at 44dB. Futher after the amplifier a four port power divider has been connected to prepare the measurement setup to connect several amplifiers. A block diagram of the setup is depicted in figure 4.1. The output of the amplifier is connected to a 31dBm attenuator to ensure that the spectrum analyser is operated under safe conditions. The signal generator generates a input signal that is a 10MHz LTE signal with a baseband frequency at 3.5GHz.

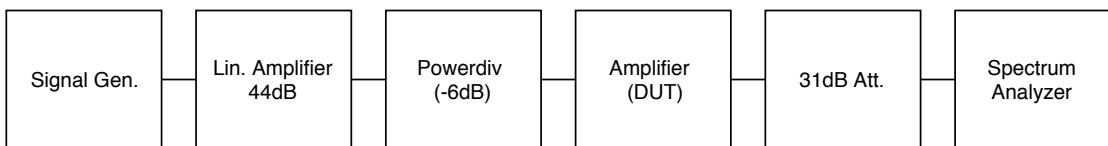


Figure 4.1: Measurement setup for measurement at only the amplifier

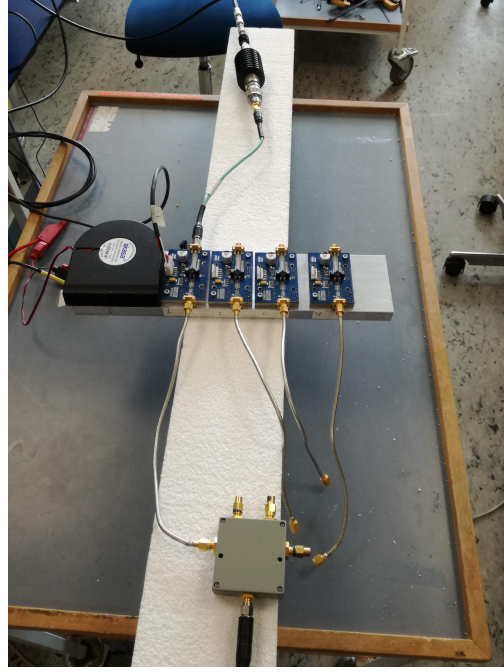


Figure 4.2: Picture of the measurement setup

In order to use DPD at the amplifier, it is important to drive the amplifier at its 1dB compression point or more. Therefore the first measurement that has to be done is to measure the gain response of the amplifier to find the input power level that satisfies this. The gate voltage for the amplifier is $V_g = 2.798V$ and the drain current is $I_d = 100mA$. The result are depicted in figure 4.3.

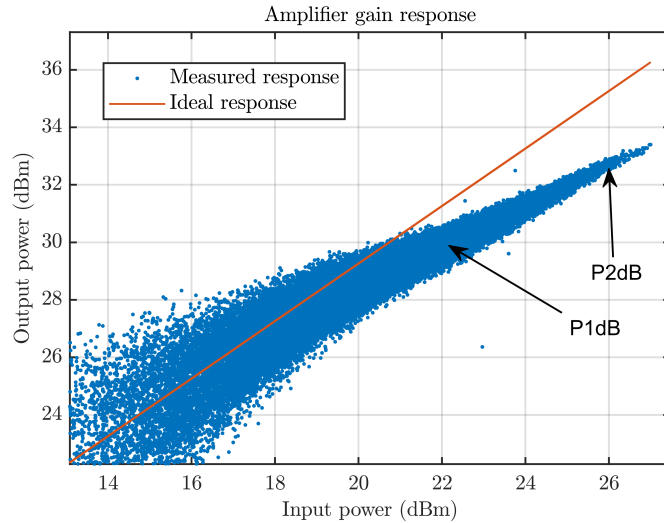


Figure 4.3: Measured gain response of the amplifier with a 10MHz LTE signal at 3.5GHz

It can be seen from figure 4.3 that the amplifier in this setup, has a gain about 10dB. The 1dB compression point is at 22dBm input power and 2dB compression is at 26dBm. It is therefore decided to continue with a power level that has a peak input power of 27dBm. The DPD algorithm has therefore been applied and the result can be seen in figure 4.4 and 4.5. It can be seen that the DPD works fine and that the distortion becomes lower with the DPD as expected. It can be seen from the AM/AM plot that the gain is lowered to 9dB with the DPD but that compression is avoided.

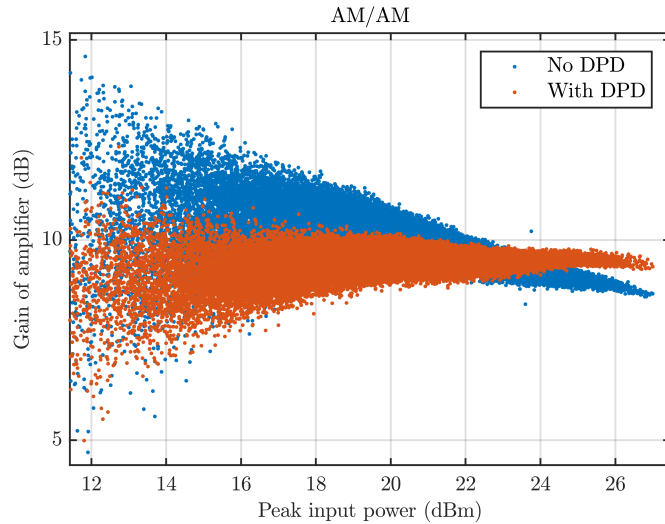


Figure 4.4: AM/AM response of the amplifier with and without DPD

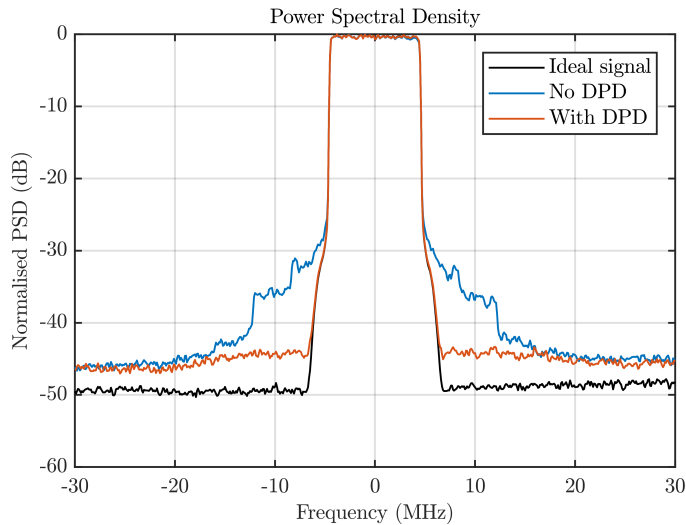


Figure 4.5: Measured PSD with and without DPD

4.2 One amplifier one antenna

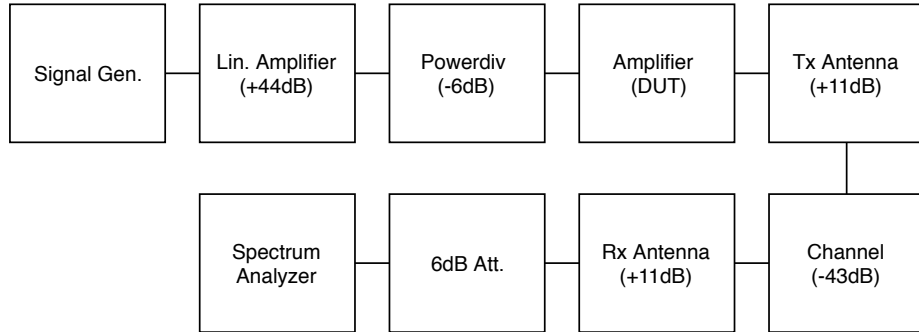


Figure 4.6: Measurement setup for measurement at one amplifier with one Tx and one Rx antenna

Since now it has been proven that the DPD works well for a single amplifier connected to a fixed load, it is necessary to see if there would be any changes when the amplifier is connected to a single Tx antenna. The measurement setup is depicted in figure 4.6. The output of the amplifier is connected to one Tx antenna with at gain at 11dB. The Rx antenna are spaced 1m apart which gives loss at 43dB in free space. The total loss can be calculated as:

$$L_{dB} = 20\log_{10}(d) + 20\log_{10}(f) + 20\log_{10}\left(\frac{4\pi}{c}\right) + G_t + G_r = 21.3dB \quad (4.1)$$

Where d is distance between the antennas, f is the center frequency, $c = 3.0e8$ is the speed of light and G_t G_r is the gain of the transmitting antenna and receiving antenna respectively [Constantine A. Balanis, 2005]. In order to compensate for the loss and to drive the spectrum analyser in the same power level as in the former measurement, the attenuator has been reduced to 6dB. It is seen from figure 4.8 that the gain now is close to 10dB which is caused by the compensation for the free space loss that is not correct but close. The distortion seen in figure 4.9 is lowered with DPD and therefore it can be concluded that the DPD still works with one antenna connected to the amplifier. The model used for DPD is the model for the amplifier only.

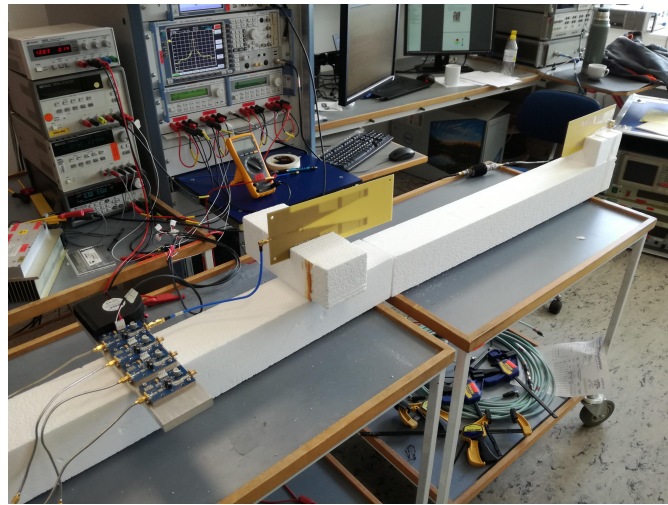


Figure 4.7: Picture of the measurement setup for one amplifier with one Tx and one Rx antenna

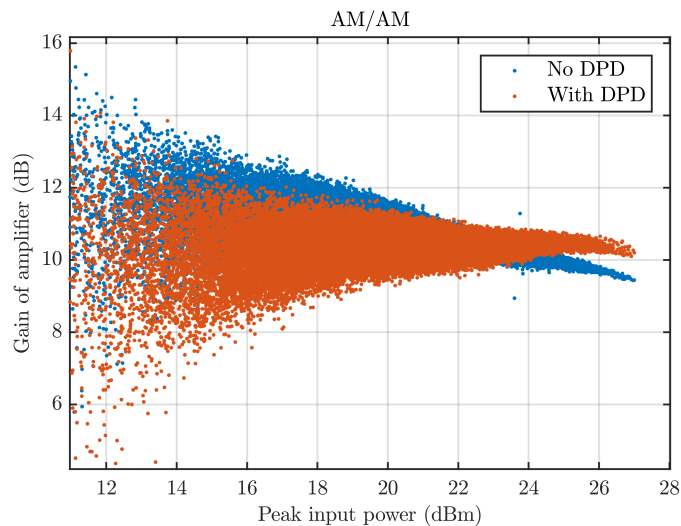


Figure 4.8: AM/AM response of the amplifier with and without DPD using one Tx antenna

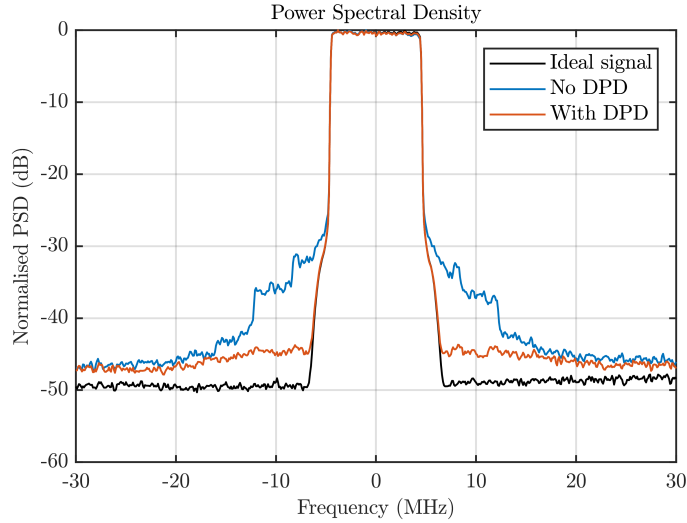


Figure 4.9: Measured PSD with and without DPD using one Tx antenna

4.3 Two amplifiers two antennas

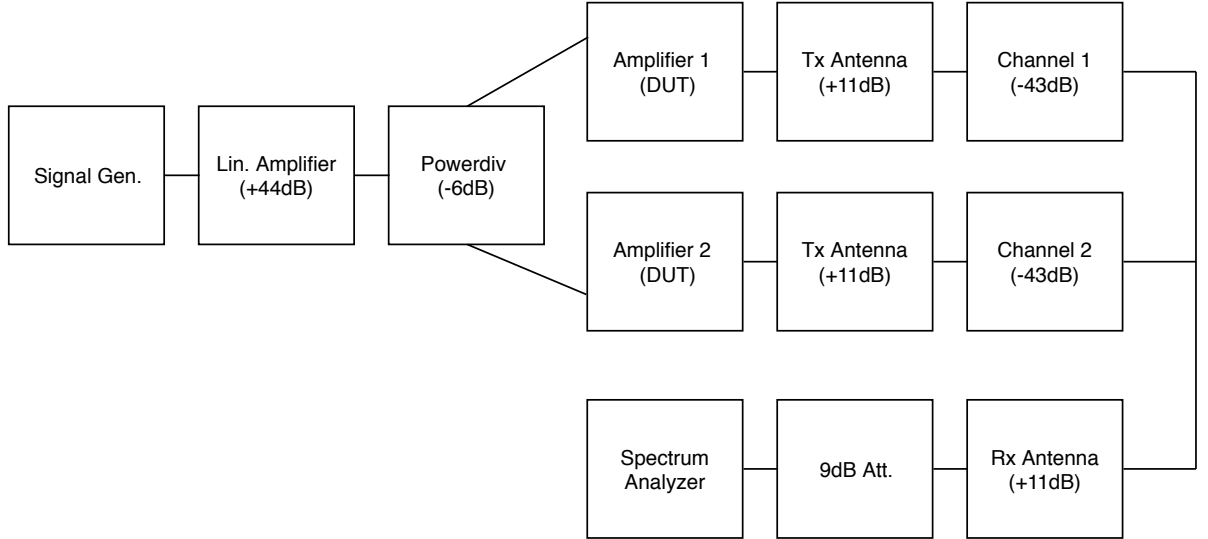


Figure 4.10: Measurement setup for measurement at two amplifiers with two Tx and one Rx antenna

In this section it is measured if it has an impact if two amplifiers are connected to an antenna each, spaced at different distances. The measurement setup is depicted in figure 4.10. Since the extra amplifier and antenna will introduce 3dB more power, 3dB is added to the attenuator to ensure the same power level at the input to the

spectrum analyzer. The measurements has all been done at the same powerlevel but the distances of the antennas are varied from 0.1 wavelength to 0.6 in steps of 0.1. First a measurement of the system is done without DPD for all distances, where the measured signal is imported into MATLAB and an inverse signal is generated. This inverse signal is then uploaded to the signal generator and the new measurement is called "With sys DPD" for each distance. Then a measurement with the inverse signal in the former section is applied for each distance and the measured signal is then called "With amp DPD".The results can be seen from figure 4.12 to 4.19.

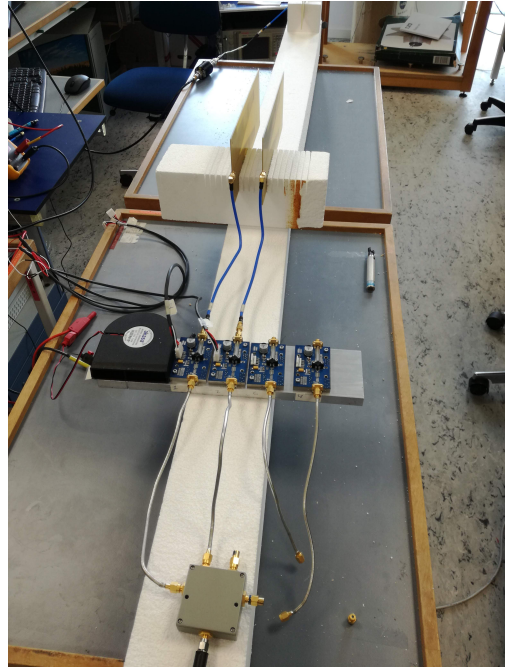


Figure 4.11: Picture of measurement setup using two Tx antennas

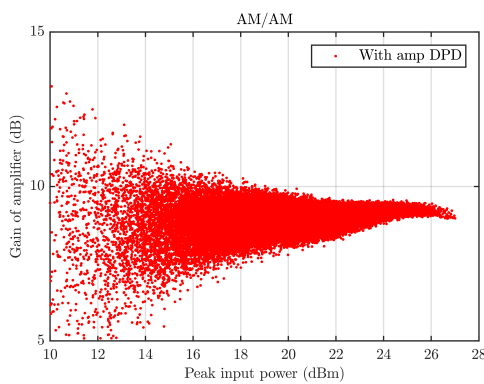


Figure 4.12: AM/AM distortion at $d = 0.1\lambda$ with amplifier DPD

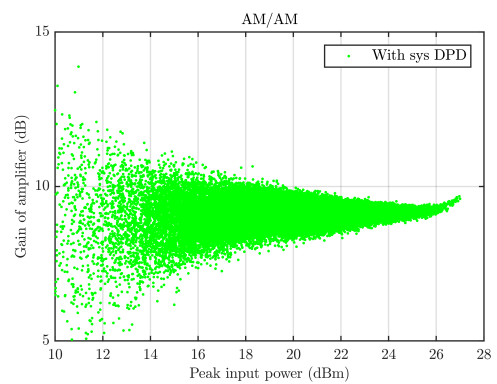


Figure 4.13: AM/AM distortion at $d = 0.1\lambda$ with system DPD

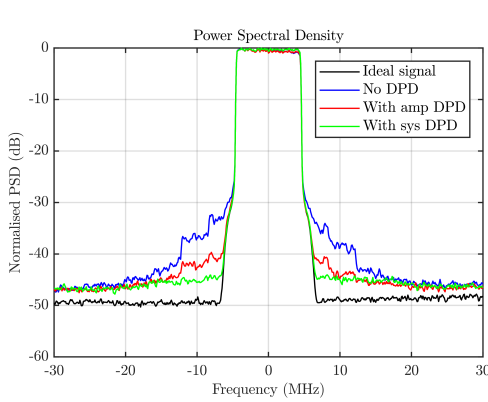


Figure 4.14: PSD of measurement at $d = 0.1\lambda$

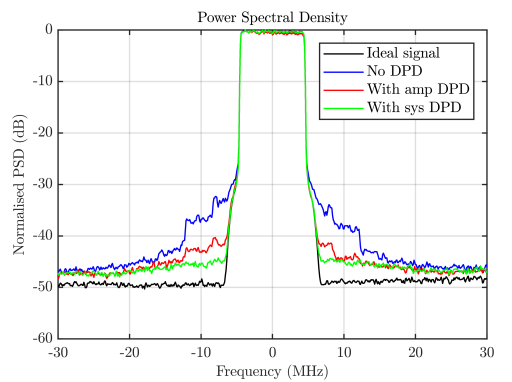


Figure 4.15: PSD of measurement at $d = 0.2\lambda$

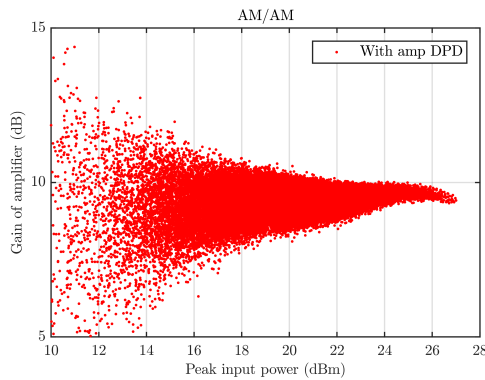


Figure 4.16: AM/AM distortion at $d = 0.2\lambda$ with amplifier DPD

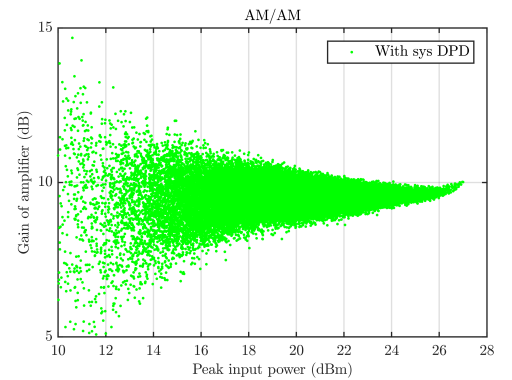


Figure 4.17: AM/AM distortion at $d = 0.2\lambda$ with system DPD

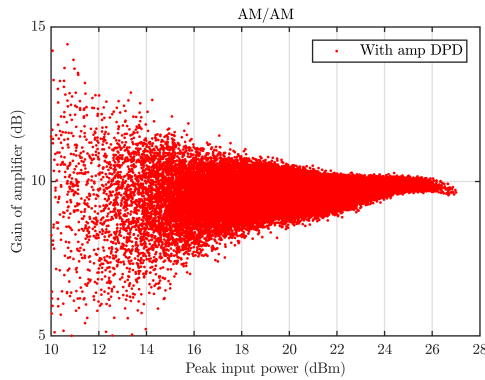


Figure 4.18: AM/AM distortion at $d = 0.3\lambda$ with amplifier DPD

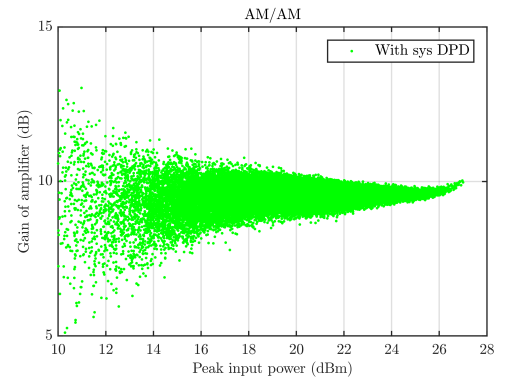


Figure 4.19: AM/AM distortion at $d = 0.3\lambda$ with system DPD

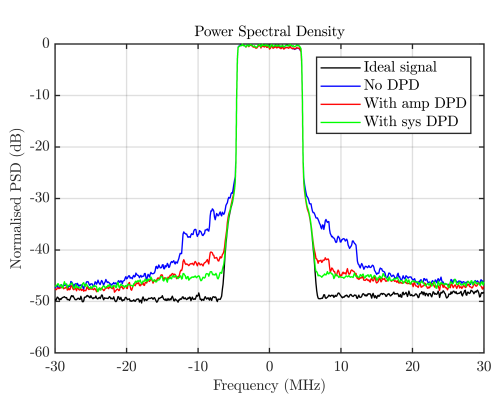


Figure 4.20: PSD of measurement at $d = 0.3\lambda$

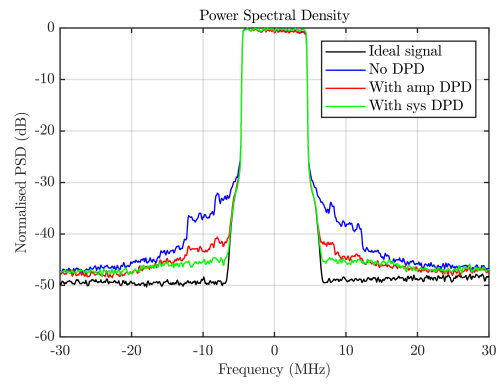


Figure 4.21: PSD of measurement at $d = 0.4\lambda$

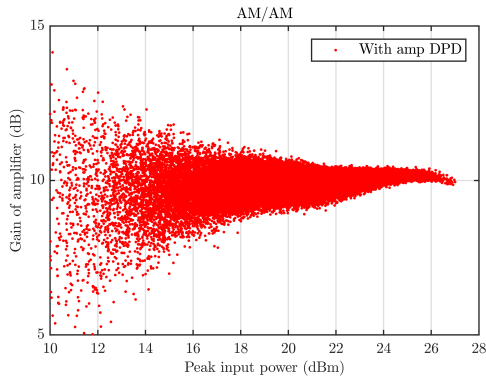


Figure 4.22: AM/AM distortion at $d = 0.4\lambda$ with amplifier DPD

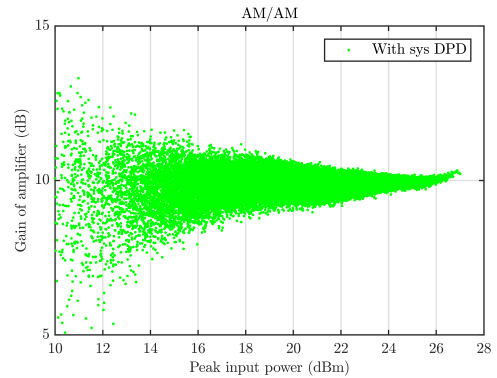


Figure 4.23: AM/AM distortion at $d = 0.4\lambda$ with system DPD

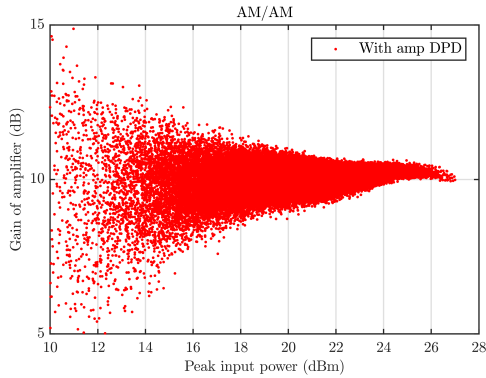


Figure 4.24: AM/AM distortion at $d = 0.5\lambda$ with amplifier DPD

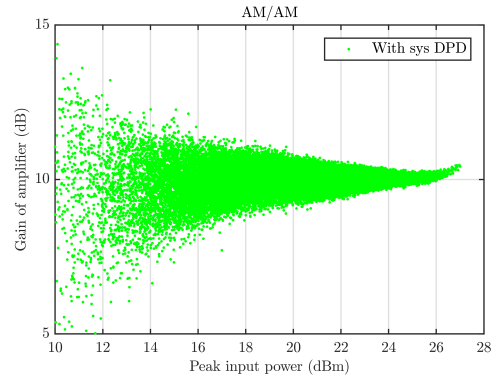


Figure 4.25: AM/AM distortion at $d = 0.5\lambda$ with system DPD

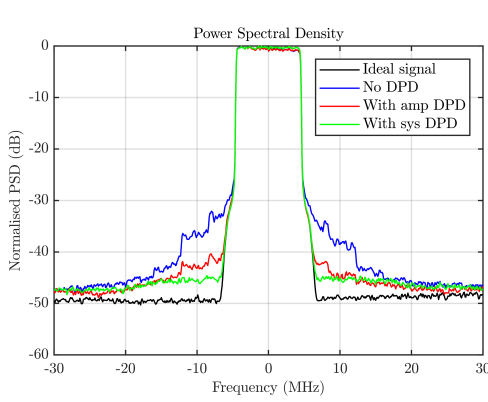


Figure 4.26: PSD of measurement at $d = 0.5\lambda$

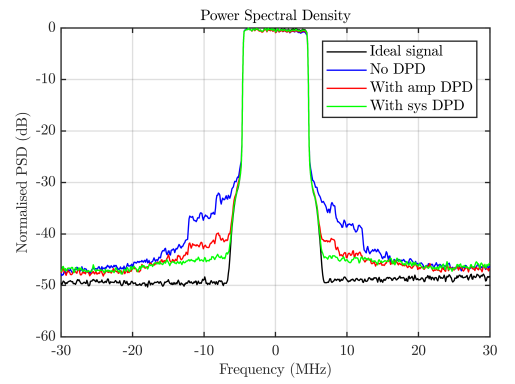


Figure 4.27: PSD of measurement at $d = 0.6\lambda$

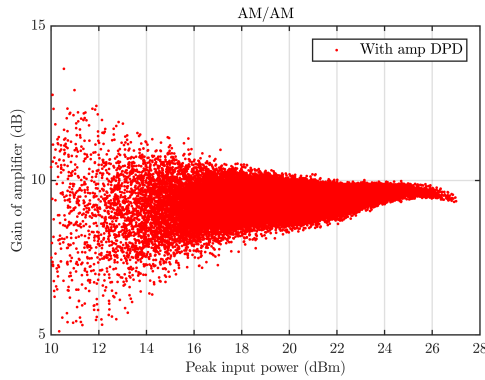


Figure 4.28: AM/AM distortion at $d = 0.6\lambda$ with amplifier DPD

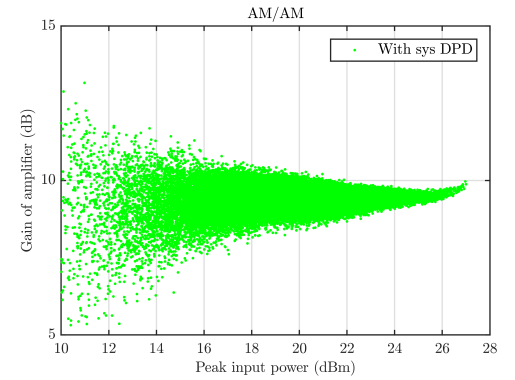
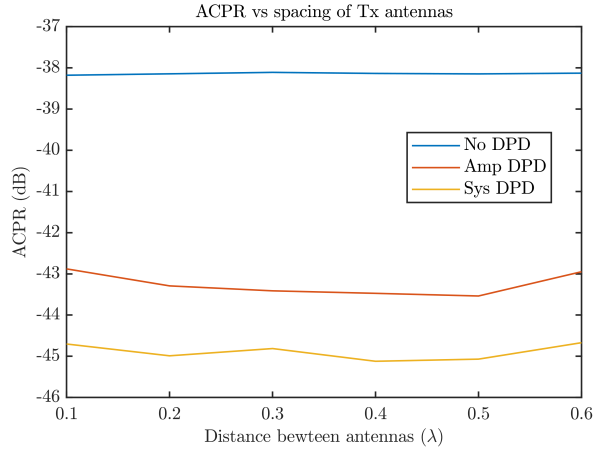


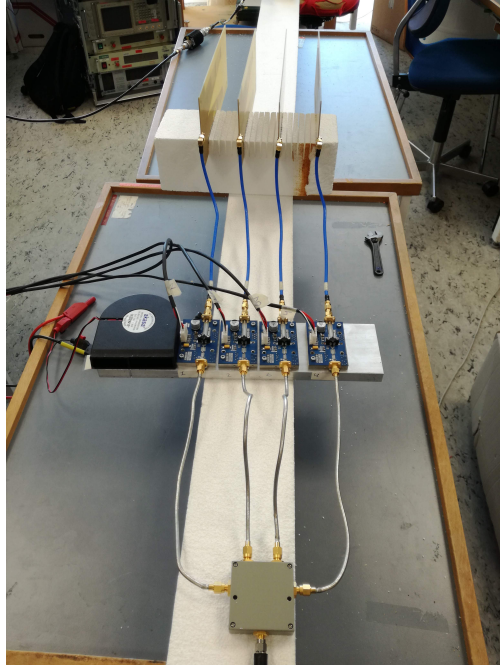
Figure 4.29: AM/AM distortion at $d = 0.6\lambda$ with system DPD

From the AM/AM plots it can be seen that when doing DPD with only the model for the amplifier taken into account, there are lots of non-linearity about 22-27dBm input. When treating the two amplifiers with antennas as one model the AM/AM linearity is improved but it seems that the DPD algorithm tends to overcompensate at high power values. From the PSD plots it is seen that the ACPR is decreased when treating the setup as one model.

**Figure 4.30:** ACPR versus distance between antennas

4.4 Four amplifiers four antennas

In this section measurement is done at four amplifiers and four antennas. The setup for the measurement is the same as in figure 4.6 but with four amplifier chains instead of two. The results are shown in figure 4.31 to 4.49.

**Figure 4.31:** Picture of measurement setup using four Tx antennas

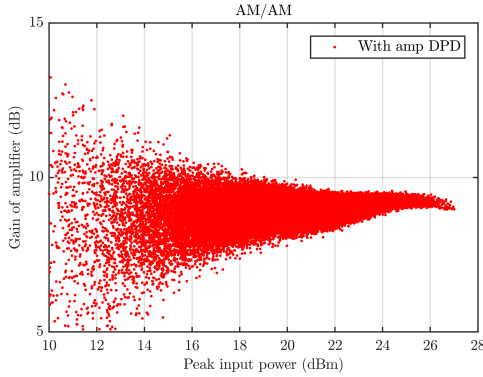


Figure 4.32: AM/AM distortion at $d = 0.1\lambda$ with amplifier DPD

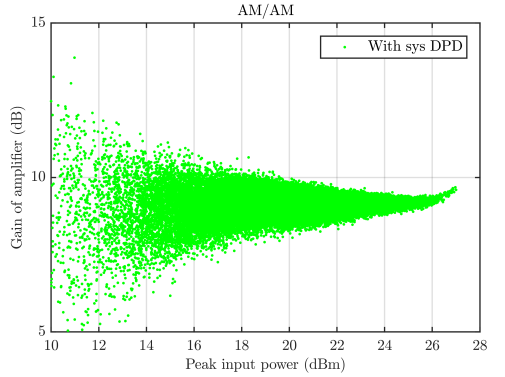


Figure 4.33: AM/AM distortion at $d = 0.1\lambda$ with system DPD

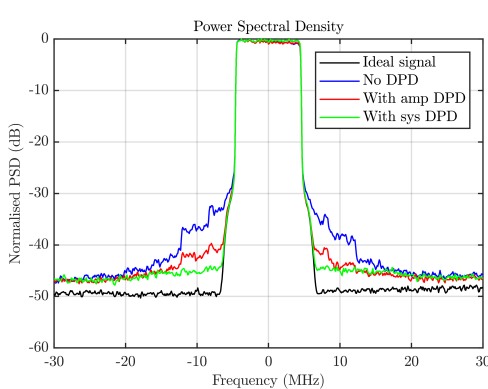


Figure 4.34: PSD of measurement at $d = 0.1\lambda$

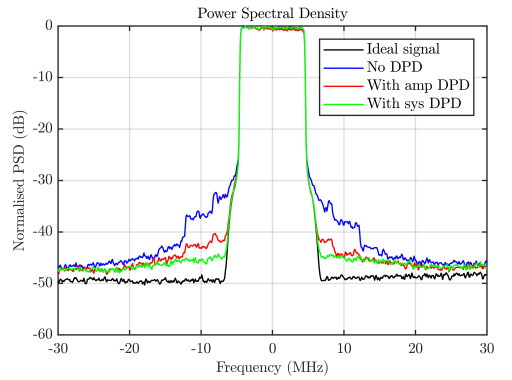


Figure 4.35: PSD of measurement at $d = 0.2\lambda$

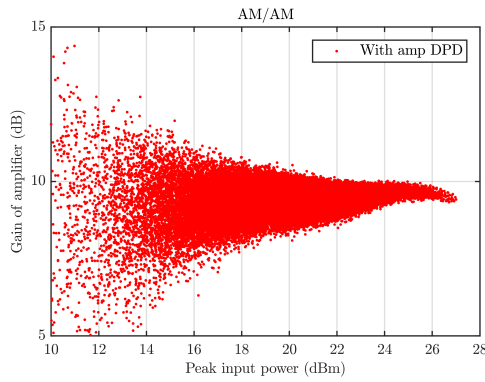


Figure 4.36: AM/AM distortion at $d = 0.2\lambda$ with amplifier DPD

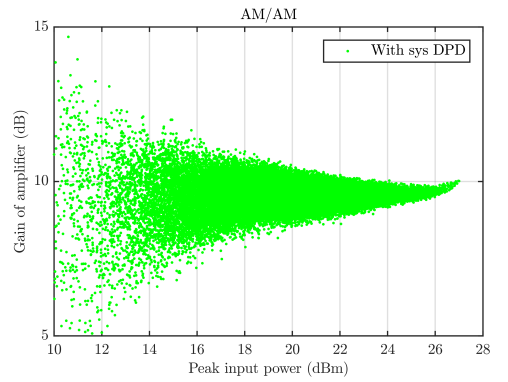


Figure 4.37: AM/AM distortion at $d = 0.2\lambda$ with system DPD

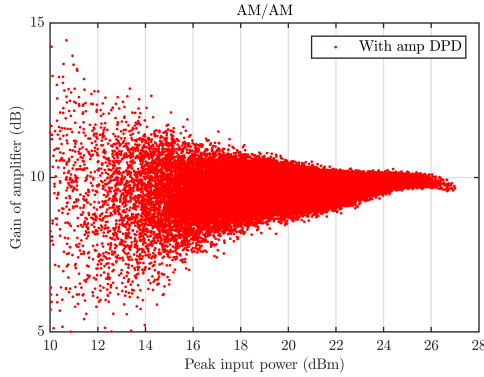


Figure 4.38: AM/AM distortion at $d = 0.3\lambda$ with amplifier DPD

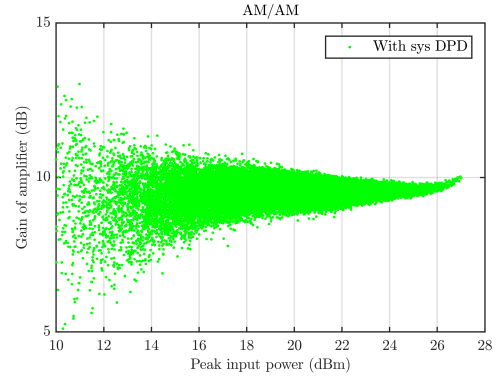


Figure 4.39: AM/AM distortion at $d = 0.3\lambda$ with system DPD

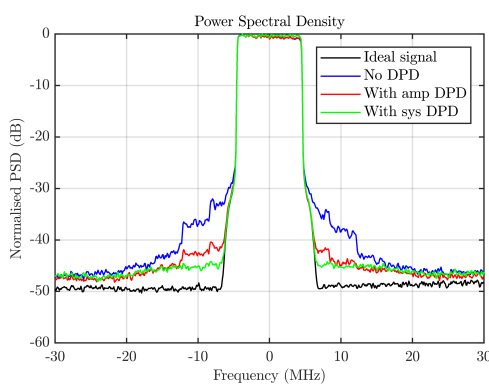


Figure 4.40: PSD of measurement at $d = 0.3\lambda$

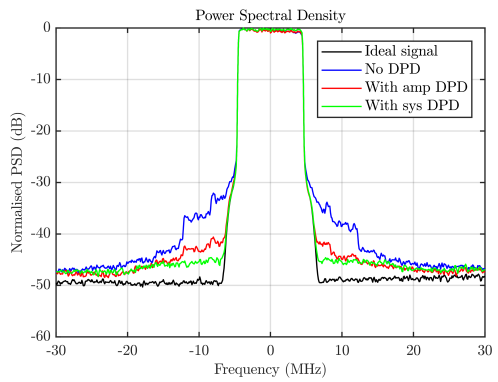


Figure 4.41: PSD of measurement at $d = 0.4\lambda$

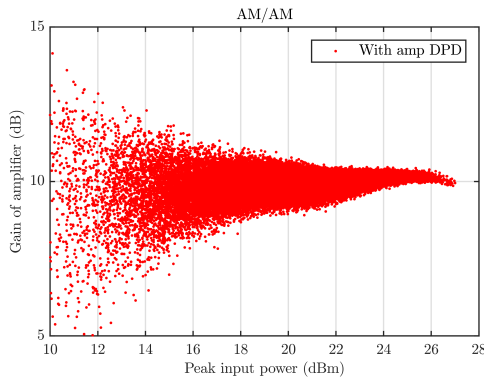


Figure 4.42: AM/AM distortion at $d = 0.4\lambda$ with amplifier DPD

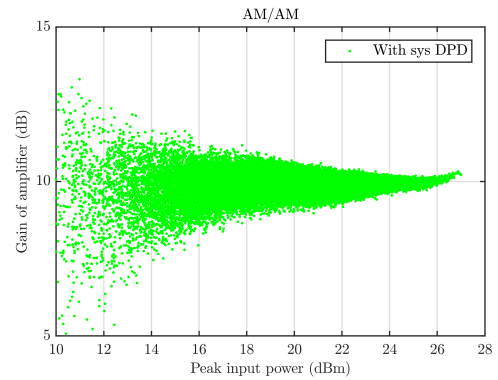


Figure 4.43: AM/AM distortion at $d = 0.4\lambda$ with system DPD

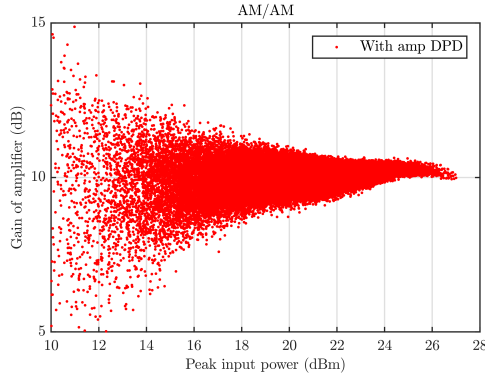


Figure 4.44: AM/AM distortion at $d = 0.5\lambda$ with amplifier DPD

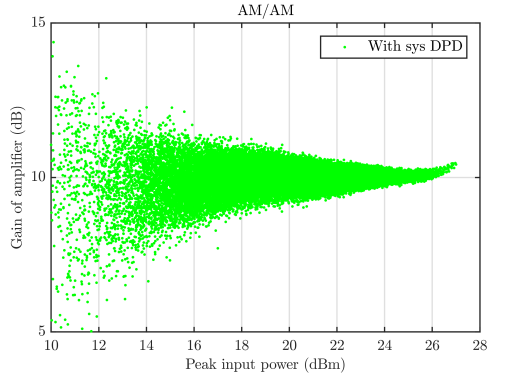


Figure 4.45: AM/AM distortion at $d = 0.5\lambda$ with system DPD

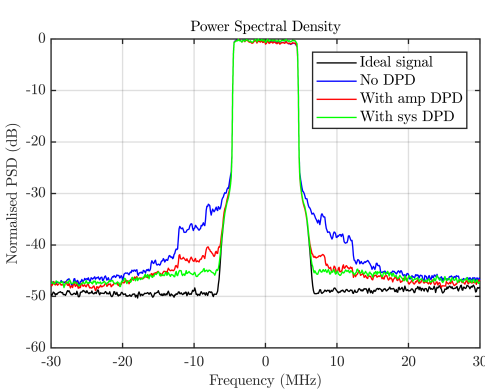


Figure 4.46: PSD of measurement at $d = 0.5\lambda$

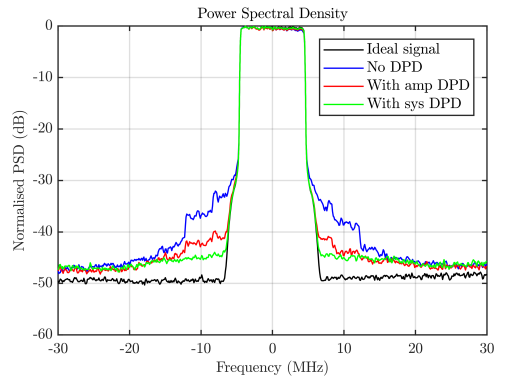


Figure 4.47: PSD of measurement at $d = 0.6\lambda$

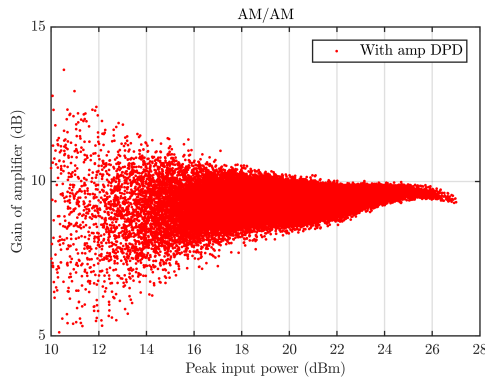


Figure 4.48: AM/AM distortion at $d = 0.6\lambda$ with amplifier DPD

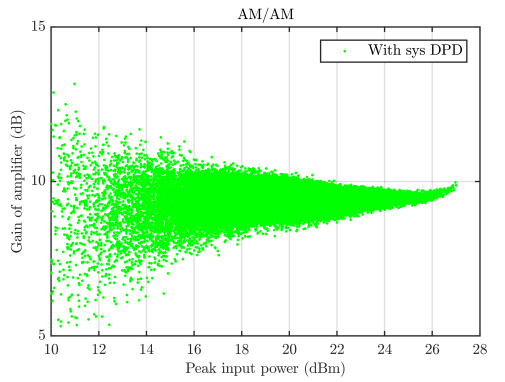


Figure 4.49: AM/AM distortion at $d = 0.6\lambda$ with system DPD

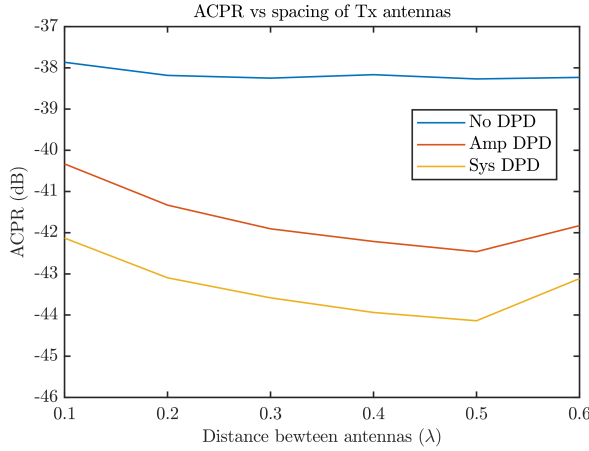


Figure 4.50: ACPR versus distance between antennas

4.5 Two amplifiers different current

In the former measurement the drain current for each amplifier has been adjusted to 100mA by tuning the gate voltage, to ensure same working conditions for all four amplifiers. In this section is measured if it has any impact that the current is different. First all four amplifiers is connected to the same gate voltage and the current is measured in each amplifier. The two amplifiers with the largest difference is then used for these measurement. The results are shown in figure 4.52 to 4.59 which shows that when the gate voltage is adjusted the performance of the amplifiers changes. This is seen at the AM/AM plots where a difference clearly is seen. This is also why DPD with only considering one amplifier as a model not can be used for multiple amplifiers if the current is different. The results shows thou that if the amplifiers with antennas are treated as a hole, then the DPD algorithm works well and therefore a different bias current is not a huge problem when doing so.

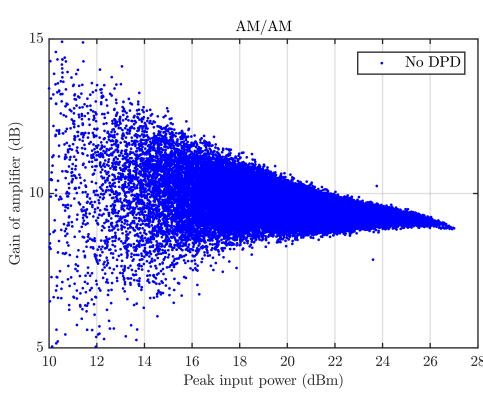


Figure 4.51: AM/AM distortion at 56mA in amplifier 1 and 100mA in amplifier 2 with gate voltages at 2.798V without DPD

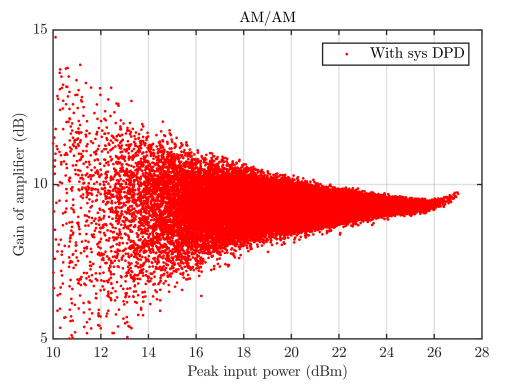


Figure 4.52: AM/AM distortion at 56mA in amplifier 1 and 100mA in amplifier 2 with gate voltages at 2.798V with DPD

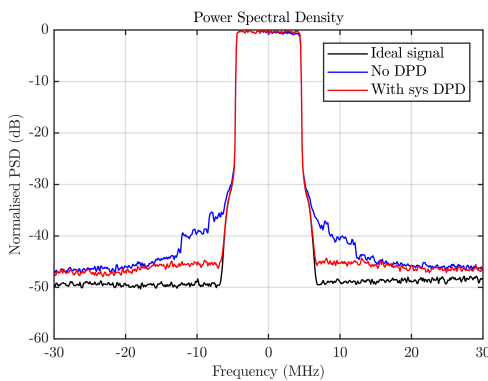


Figure 4.53: PSD at 56mA in amplifier 1 and 100mA in amplifier 2 with gate voltages at 2.798V

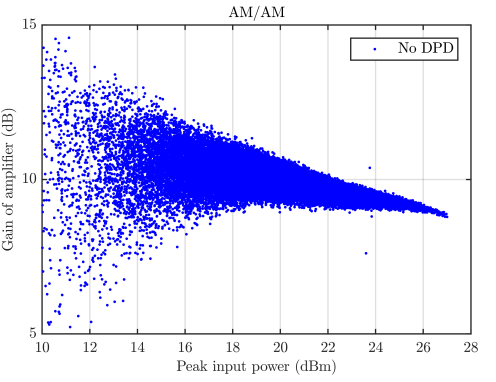


Figure 4.54: AM/AM distortion at 75mA in amplifier 1 and 112mA in amplifier 2 with gate voltages at 2.742V without DPD

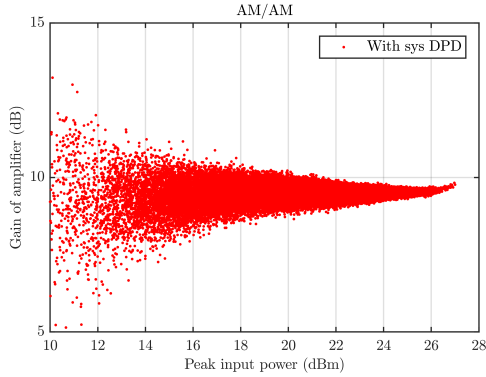


Figure 4.55: AM/AM distortion at 75mA in amplifier 1 and 112mA in amplifier 2 with gate voltages at 2.742V with DPD

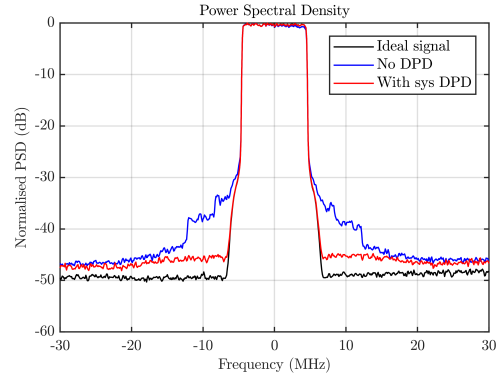


Figure 4.56: PSD at 75mA in amplifier 1 and 112mA in amplifier 2 with gate voltages at 2.742V

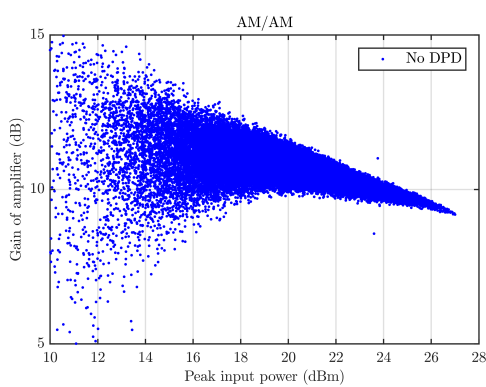


Figure 4.57: AM/AM distortion at 100mA in amplifier 1 and 136mA in amplifier 2 with gate voltages at 2.672V without DPD

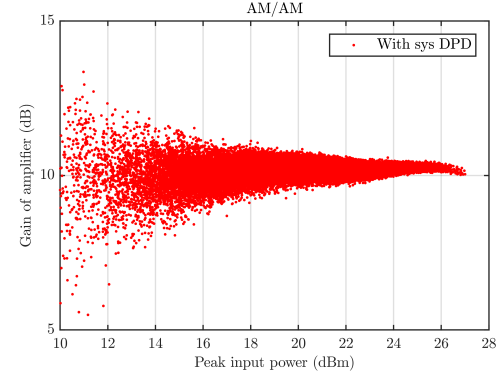


Figure 4.58: AM/AM distortion at 100mA in amplifier 1 and 137mA in amplifier 2 with gate voltages at 2.672V with DPD

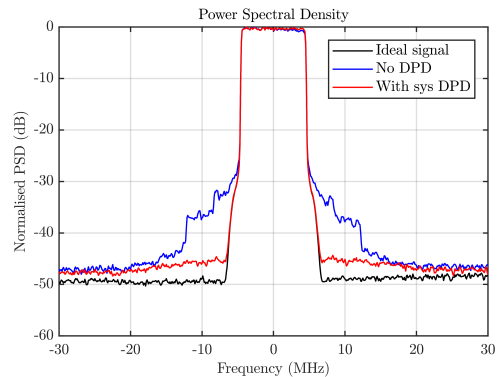


Figure 4.59: PSD at 100mA in amplifier 1 and 137mA in amplifier 2 with gate voltages at 2.672V

Chapter 5

Antenna measurement

5.1 Single antenna

The first measurement done is the farfield of a single antenna only. The measurement of the farfield is done in an anechoic chamber to ensure that no reflections will affect the results. See figure 5.1 The antenna is mounted on a fixture made of flamingo and is connected directly to a cable that further is connected to a signal generator. The measurement shows in figure 5.2 that the antenna has a maximum gain at 11.1 dB and that the farfield can be assumed omnidirectional. The S-paramerets has also been measured but those are not done in an anechoic chamber, but at a setup that is depicted in figure 5.34 the reason is that it was not possible to do the measurement in an anechoic chamber because of the network analyzer who was fixed in an other room. The best would have been to first measure the S-parameters in the anechoic chamber and then measure the S-parameters in the setup where the mesaurement with the amplifiers has been done to see the differences when introducing reflections from the room. Since this has not been possible both due to time and equipment one should be aware of the eventually differences.

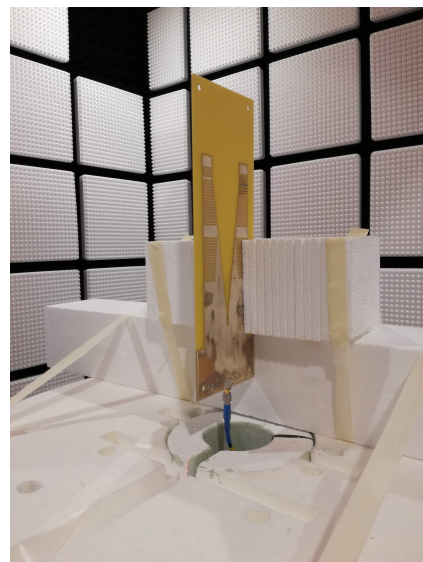


Figure 5.1: Measurement of a single antenna in an anechoic chamber

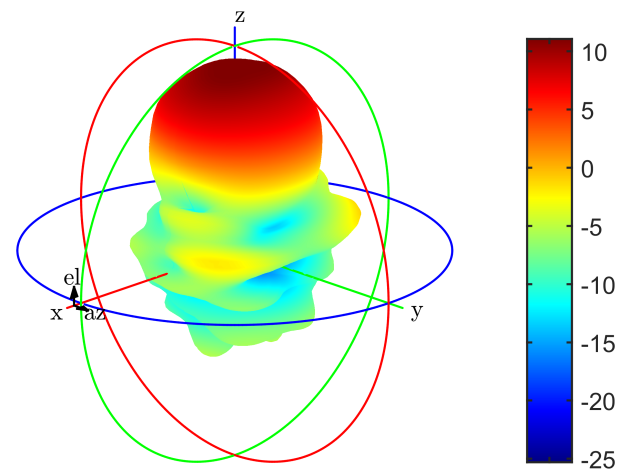


Figure 5.2: Measured farfield in dB. Maximum gain is 11.1dB

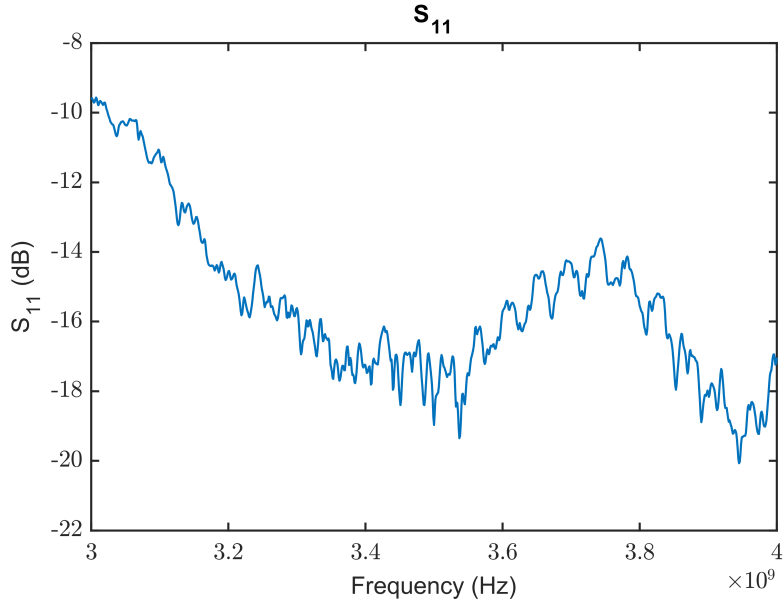


Figure 5.3: Measured S11 parameter of a single antenna

5.2 Two antennas

In this section measurement is done at two antennas that are spaced at different distances. This is to see how the farfield will change due to coupling of the array. In the theory the gain should become 3dB greater using two antennas than using one antenna, but for this measurement a power divider is used, which is a 4-port divider that introduces a loss at 6dB to every port. Therefore a decrease of 3dB is expected. The unused ports of the power divider is terminated to a 50Ω load. It is seen from figure 5.5 to 5.10 that the farfield flattens in the y direction and that the gain varies with the distances between the elements. The loss seems to be lower than expected since a loss at only 2.2dB is obtained at $d = 0.5\lambda$. The S-parameters is presented in figure 5.11 to 5.14. It is seen that as expected S_{11} and S_{22} are similar and that S_{12} and S_{21} also are similar. It is seen that the return-loss S_{11} and S_{22} changes a lot with the spacing of the antennas. The largest difference is seen from 0.1 to 0.3 wavelengths. This is also seen from the coupling S_{12} and S_{21} that at 0.1 and 0.2 wavelengths ther is a large amount of coupling.

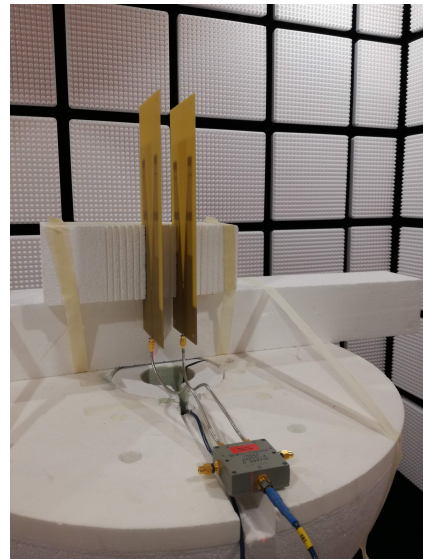


Figure 5.4: Measurement of two antennas with a powerdivider in an anechoic chamber. The distances between the antennas are varied for every measurement. The distance is 0.5λ on the picture



Figure 5.5: Farfield for $d = 0.1\lambda$. Maximum gain is 7.8dB

Figure 5.6: Farfield for $d = 0.2\lambda$. Maximum gain is 8.2dB

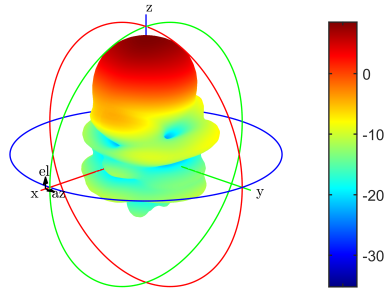


Figure 5.7: Farfield for $d = 0.3\lambda$. Maximum gain is 8.5dB

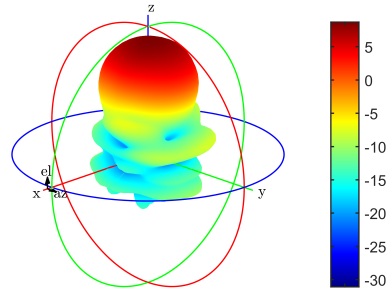


Figure 5.8: Farfield for $d = 0.4\lambda$. Maximum gain is 8.7dB

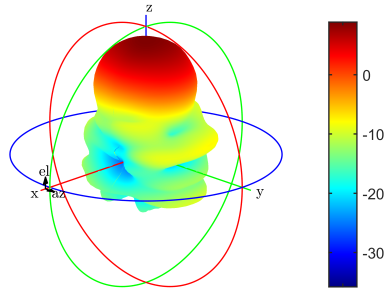


Figure 5.9: Farfield for $d = 0.5\lambda$. Maximum gain is 8.9dB

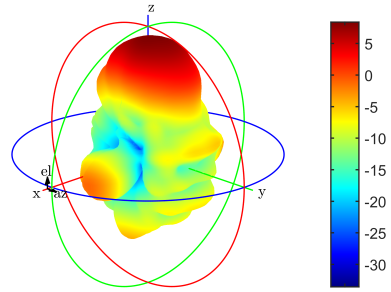


Figure 5.10: Farfield for $d = 0.6\lambda$. Maximum gain is 8.4dB

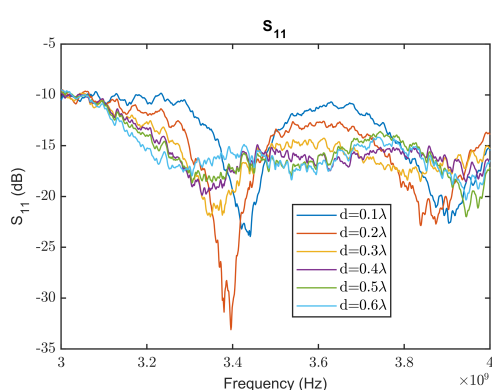


Figure 5.11: Measured S_{11} with two antennas

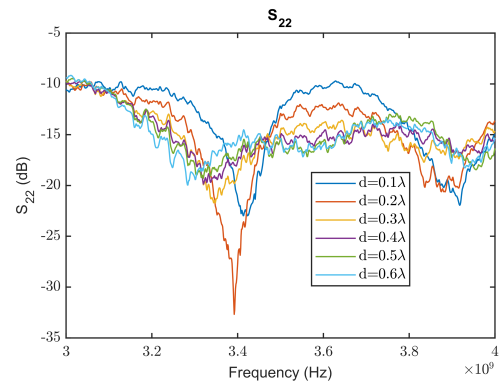


Figure 5.12: Measured S_{22} with two antennas

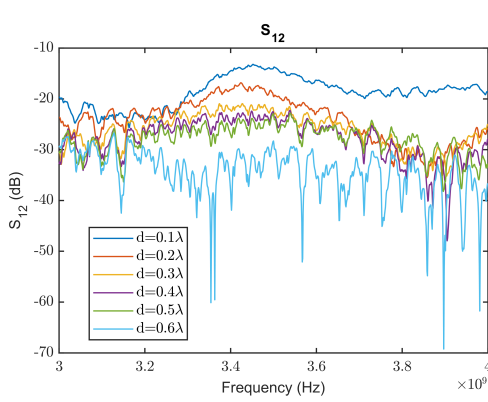


Figure 5.13: Measured S_{12} with two antennas

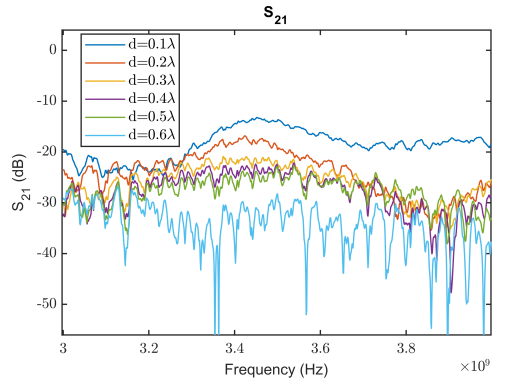


Figure 5.14: Measured S_{21} with two antennas

5.3 Four antennas

In this section four antennas is measured. The expected gain is the same as for one antenna because of the powerdivider. Like the case for the measurement done at two antennas the distances is also varied in these measurements. The unused antennas are terminated to 50Ω . It is seen that the farfield flattens even more at this configuration in the y axis. This is mainly caused by the geometry of the antennas. The gain is also higher then expected which can be seen from figure 5.16 to 5.21. The S-parameters are presented in figure 5.22 to 5.33. The S-parameters shows that S_{11} and S_{44} are similar and that S_{22} and S_{33} are similar thou variations is seen. This is mainly because that the distance between the antennas are not exactly the same ant that the antennas in them self have small variations. Like in the case with two antennas the coupling gets worse with a smaller distance ant the return loss also variates a lot.



Figure 5.15: Measurement of four antennas with a powerdivider in an anechoic chamber. The distances between the antennas are varied for every measurement. The distance is 0.5λ on the picture

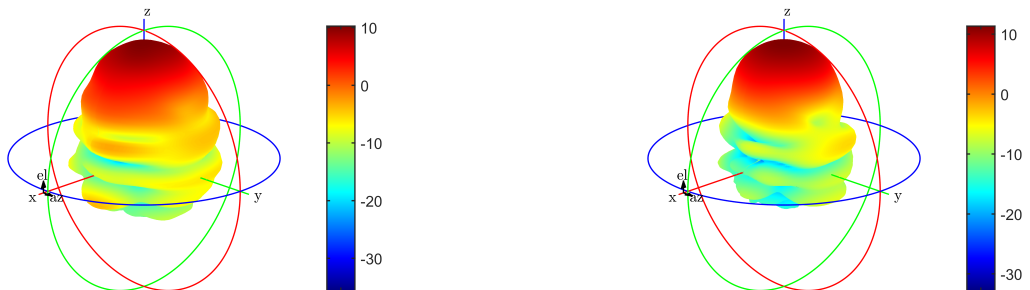


Figure 5.16: Farfield for $d = 0.1\lambda$. Maximum gain is 10.3dB

Figure 5.17: Farfield for $d = 0.2\lambda$. Maximum gain is 11.3dB



Figure 5.18: Farfield for $d = 0.3\lambda$. Maximum gain is 12.2dB

Figure 5.19: Farfield for $d = 0.4\lambda$. Maximum gain is 13.1dB

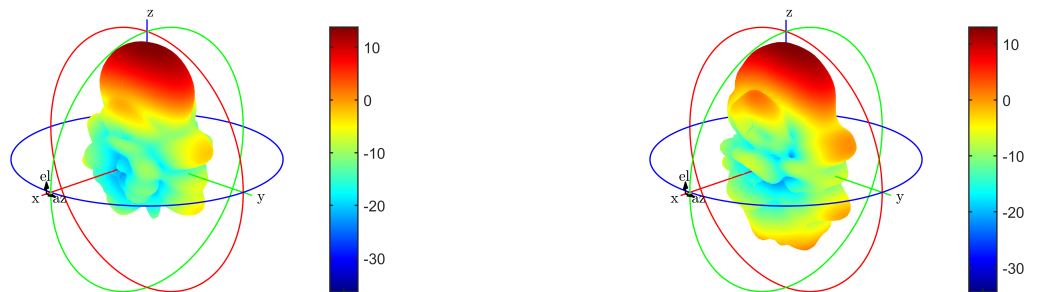


Figure 5.20: Farfield for $d = 0.5\lambda$. Maximum gain is 13.8dB

Figure 5.21: Farfield for $d = 0.6\lambda$. Maximum gain is 13.0dB

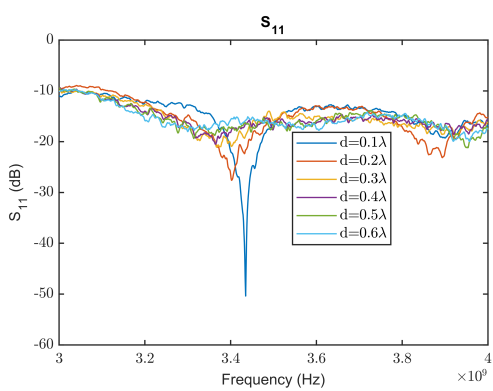


Figure 5.22: Measured S_{11} with four antennas

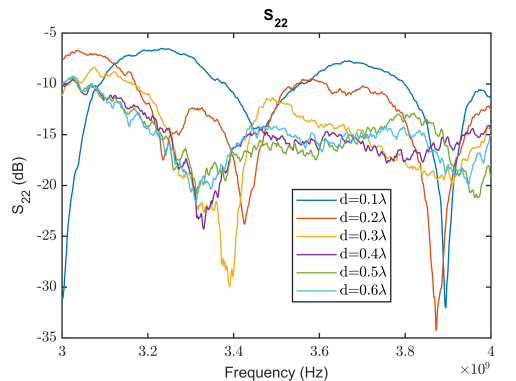
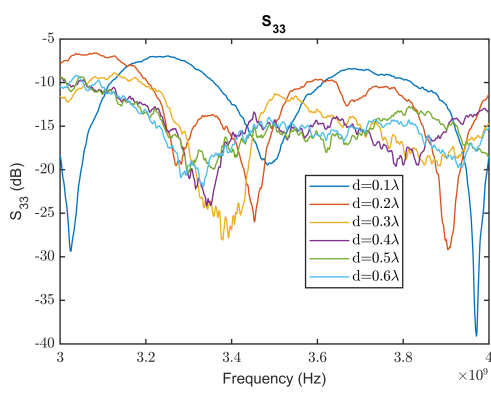
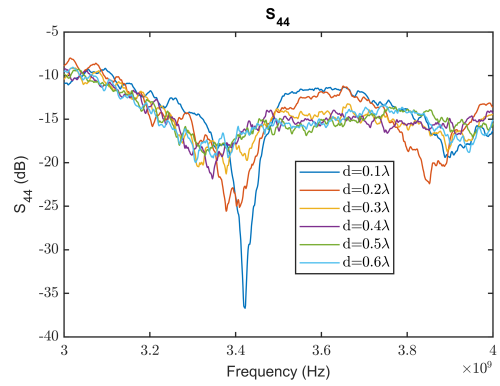
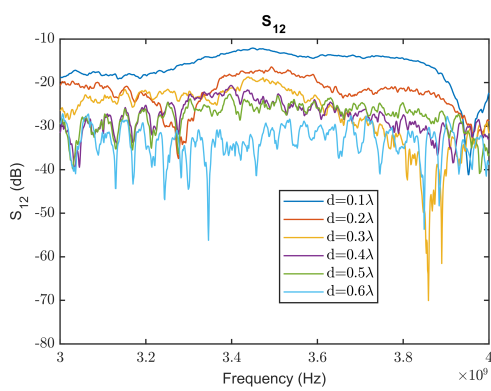
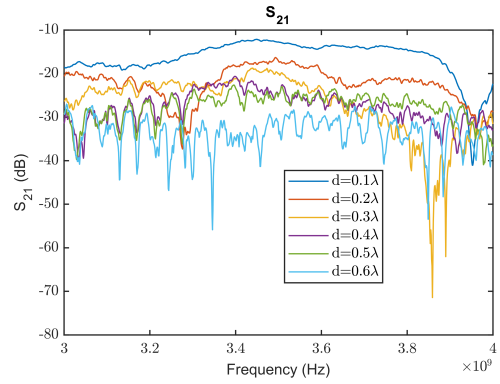
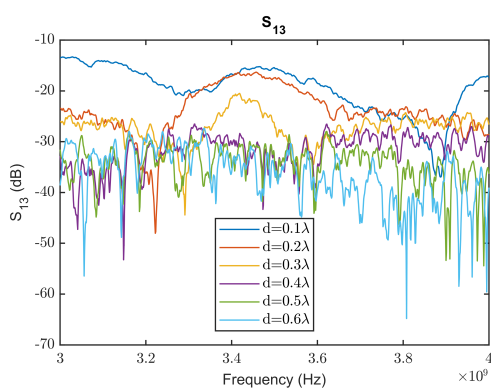
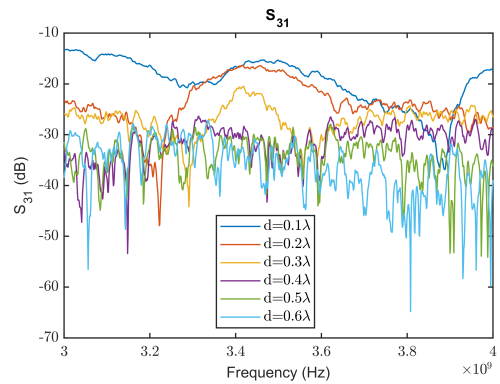


Figure 5.23: Measured S_{22} with four antennas

**Figure 5.24:** Measured S_{33} with four antennas**Figure 5.25:** Measured S_{44} with four antennas**Figure 5.26:** Measured S_{12} with four antennas**Figure 5.27:** Measured S_{21} with four antennas**Figure 5.28:** Measured S_{13} with four antennas**Figure 5.29:** Measured S_{31} with four antennas

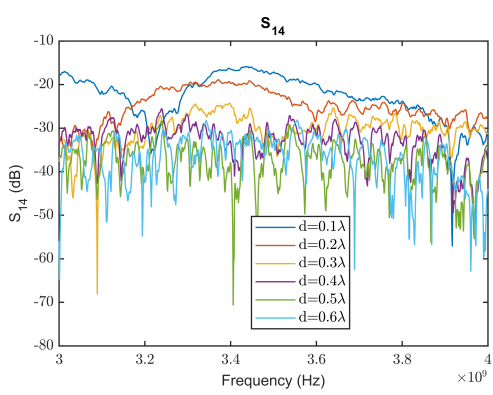


Figure 5.30: Measured S_{14} with four antennas

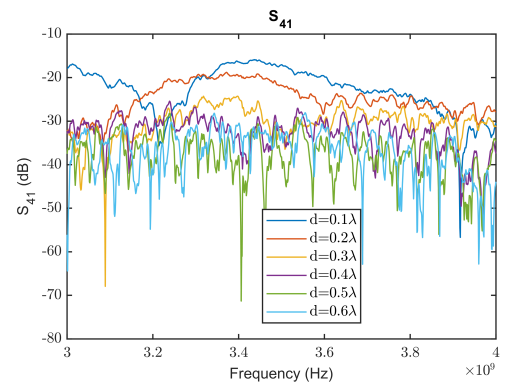


Figure 5.31: Measured S_{41} with four antennas

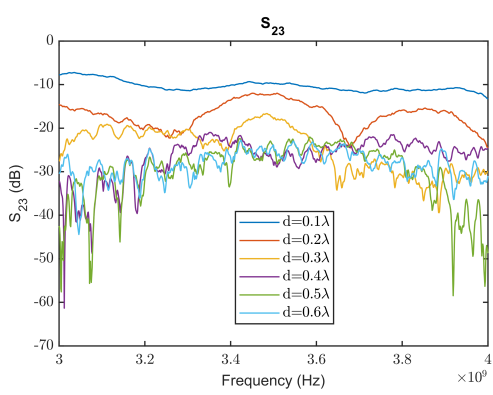


Figure 5.32: Measured S_{23} with four antennas

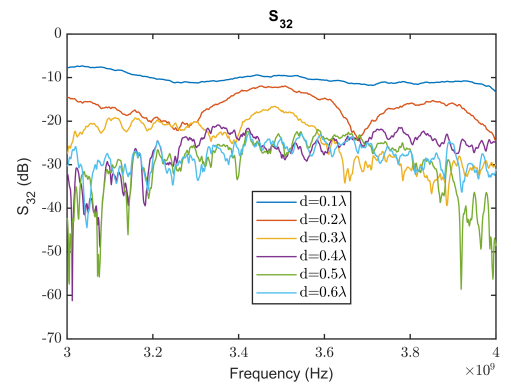


Figure 5.33: Measured S_{32} with four antennas

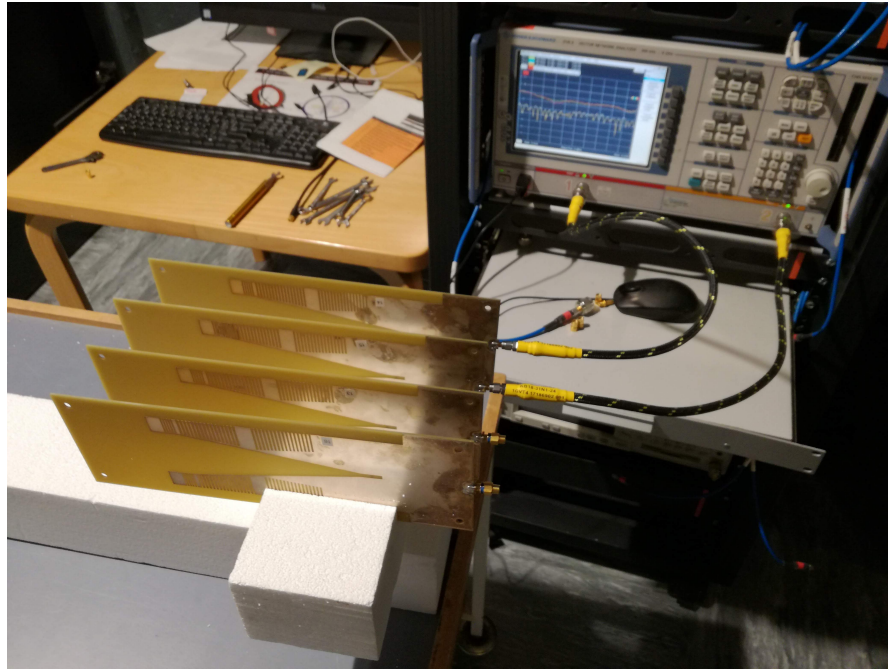


Figure 5.34: Measurement of S-parameters using four antennas. The measurement using one and two antennas has been done at the same way. The unused antennas are terminated to 50Ω

5.4 Single element four antennas

In this section the farfield of a single element in a array with 4 antennas is measured. It is expected that the first and fourth element has a radiation pattern opposite to each other and that second and the third also is opposite with each other. It is seen to be somewhat true in figure 5.36 to 5.39 thou variations is seen.

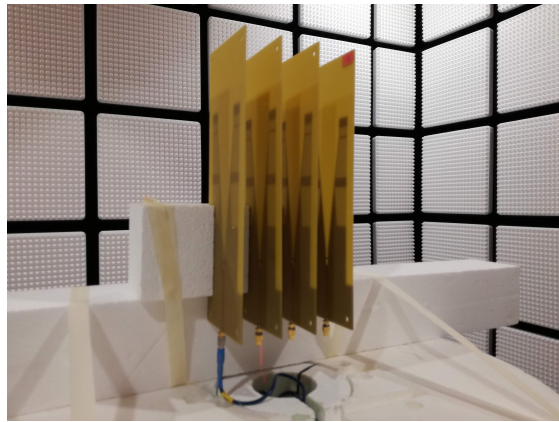


Figure 5.35: Measurement of a single antenna in a 4 element array. The unused antennas is terminated to 50Ω . For every measurement the cable is mounted on another antenna and the load is shifted.

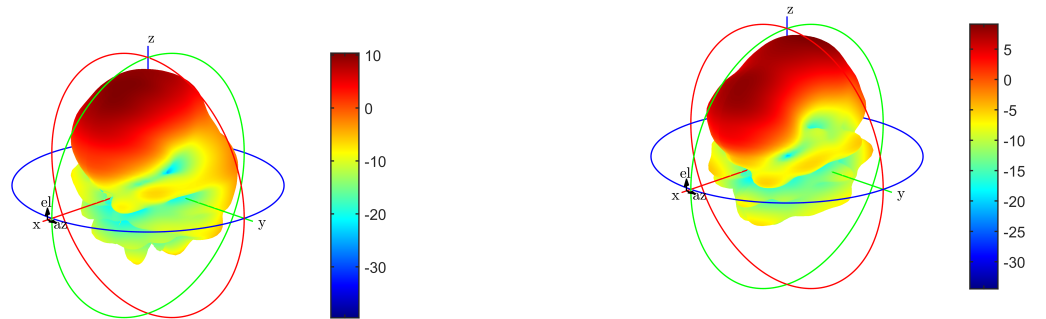


Figure 5.36: Farfield first element in the four element array. Maximum gain is 10.4dB

Figure 5.37: Farfield second element in the four element array. Maximum gain is 9.1dB

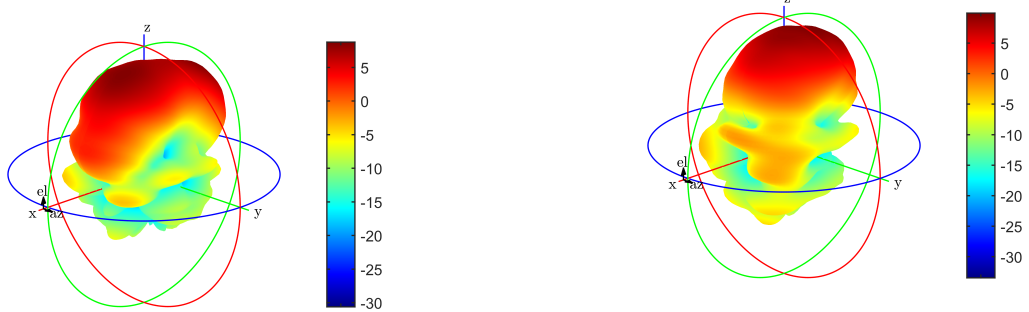


Figure 5.38: Farfield third element in the four element array. Maximum gain is 8.8dB

Figure 5.39: Farfield fourth element in the four element array. Maximum gain is 9.9dB

Chapter 6

Conclusion

The purpose of this project was to development an antenna to receive ADS-B signals from aircraft's on a CubeSat. A link budget was made and it showed that there was a need for a radiation-pattern that could compensate for the increased length in the reception due to the angle of the earth. Another important requirement for the antenna was that it should be circular-polarized since the received signal was linear polarized but the angle of reception was not known. A reflector antenna, a quadrifilar helical antenna and a hemispherical antenna was investigated. None of these antenna could overcome those requirements in their basic forms and modifications to these was investigated. The reflector antenna had a high gain in one single direction and a large size compared to the wavelength which made it difficult to use on a CubeSat. The quadrifilar helical antenna showed that is was difficult to change in its radiation-pattern due to the common design and still keep it circular polarized. The hemispherical helical antenna was modified to have four arms and a stretched structure which showed good performance, but this design had no gain in the center. This could be improved by changing the feeding point, but this introduced a non-symmetry which made the antenna to become non circular polarized.

Bibliography

Ali Cheaito, et. al (2016). Evm derivation of multicarrier signals to determine the operating point of the power amplifier considering clipping and predistortion. ResearchGate.

Andreas F. Molisch (2011). *Wireless Communications*. Wiley, 2. ed. edition.

Constantine A. Balanis (2005). *Antenna Theory Analysis And Design*. Wiley, 3. ed. edition.

Katharina Hausmair, et. al (2017). Digital predistortion for multi-antenna transmitters affected by antenna crosstalk. http://www.ieee.org/publications_standards/publications/rights/index.html.

National Instruments (2019). Optimizing ip3 and acpr measurements. www.ni.com/rf-academy.

Silvus Technologies (2019). Introduction to mimo. <https://silvustechologies.com/why-silvus/technology/introduction-to-mimo/>.

Taijun Liu, et.al (2007). Memory effect pre-compensation for wideband rf power amplifiers using fir-based weak nonlinear filters. <https://ieeexplore.ieee.org>.

Xuan Wang, et. al (2011). Correlation coefficient expression by s-parameters for two omni-directional mimo antennas. <https://ieeexplore.ieee.org/stamp/stamp.jsp?arnumber=5996702>.

Yan Guo, et.al (2015). Power adaptive digital predistortion for wideband rf power amplifiers with dynamic power transmission. IEEE TRANSACTIONS ON MICROWAVE THEORY AND TECHNIQUES, VOL. 63, NO. 11, NOVEMBER 2015.

Zahidul Islam Shahin, et. al (2017). Efficient dpd coefficient extraction for compensating antenna crosstalk and mismatch effects in advanced antenna system. Department of Electrical and Information Technology LTH, Lund University SE-221 00 Lund, Sweden.

Appendix A

Antenna measurements